



# New Physics searches using Lepton Flavour Universality tests at LHCb

Leroy Olivier

## ► To cite this version:

| Leroy Olivier. New Physics searches using Lepton Flavour Universality tests at LHCb. 11th France  
| China Particle Physics Laboratory workshop (FCPPL2018), May 2018, Marseille, France. in2p3-  
| 01801519

**HAL Id: in2p3-01801519**

<https://hal.in2p3.fr/in2p3-01801519>

Submitted on 4 Mar 2019

**HAL** is a multi-disciplinary open access archive for the deposit and dissemination of scientific research documents, whether they are published or not. The documents may come from teaching and research institutions in France or abroad, or from public or private research centers.

L'archive ouverte pluridisciplinaire **HAL**, est destinée au dépôt et à la diffusion de documents scientifiques de niveau recherche, publiés ou non, émanant des établissements d'enseignement et de recherche français ou étrangers, des laboratoires publics ou privés.

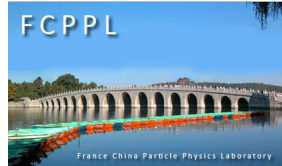
# New Physics searches using Lepton Flavour Universality tests at LHCb

Olivier Leroy, on behalf of the LHCb collaboration

Aix Marseille Univ, CNRS/IN2P3, CPPM, Marseille, France

23 May 2017

11th FCPPL Workshop, Marseille, France, 22–25 May 2018



# Outline

- 1 Introduction
- 2 LFU tests with  $b \rightarrow s\ell\ell$
- 3 LFU tests with  $b \rightarrow c\tau\nu_\tau$
- 4 Conclusions and prospects

# Flavor physics: WHAT, WHY, HOW ?

- ➊ WHAT: Quarks and leptons exist in 6 “flavors” ( $u, c, t, d, s, b$ ) and ( $e, \mu, \tau, \nu_e, \nu_\mu, \nu_\tau$ ).
- ➋ WHY:
  - Flavor is at the heart of the Standard Model, involving 22 of the 28 free parameters (masses and mixing of fundamental fermions, CP violation)
  - Flavor physics loop processes (box and penguins) are sensitive to energy scales well beyond the ones of the accelerators, thanks to virtual contributions



→ Indirect search for New Physics

- ➌ HOW:
  - Compare precise theoretical predictions with precise experimental measurements
  - LHCb, Belle, BaBar, ATLAS, CMS, NA62, BESIII, neutrinos experiments, ...!

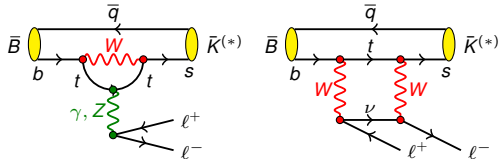
# Lepton Flavor Universality

- SM features Lepton Flavor Universality (**LFU**): equal electroweak coupling to all charged leptons. Branching ratios to  $e$ ,  $\mu$  and  $\tau$  differ only due to their mass
- However, some deviations measured already at **LEP**
$$\frac{2\sigma(W \rightarrow \tau\nu_\tau)}{\sigma(W \rightarrow e\nu_e) + \sigma(W \rightarrow \mu\nu_\mu)} = 1.077 \pm 0.026, \text{ } 2.8\sigma \text{ above SM}$$
 [arXiv:0511027]
- And more recently at *b*-factories and LHCb using semileptonic *B* decays:
$$R(D^{(*)}) = \frac{\mathcal{B}(B \rightarrow D^{(*)} - \tau^+ \nu_\tau)}{\mathcal{B}(B \rightarrow D^{(*)} - \ell^+ \nu_\ell)} \quad (\ell = \mu, e), \text{ a combined effect } 4.1\sigma \text{ above SM}$$
 [HFLAV]
- Also the rare decay observables  $R_{K^{(*)}} = \frac{\mathcal{B}(B \rightarrow K^{(*)} \mu^+ \mu^-)}{\mathcal{B}(B \rightarrow K^{(*)} e^+ e^-)}$  exhibit some tensions  $\sim 3\sigma$  below SM [PRL 113, 151601 (2014), JHEP 08 (2017) 055, JHEP 1801 (2018) 093]
- Possible BSM scenarios: leptoquarks, new heavy vector bosons,  $H^\pm$ , ...
- We will present measurements of ratios of these *B* branching ratios at LHCb:
  - Theoretically clean: cancellation of QCD effects
  - Experimentally clean: cancellation of efficiency and reconstruction effects

# In this talk: two front LFU tests

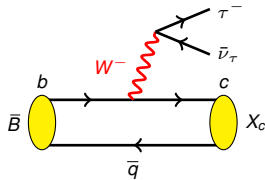
►  $R(K^{(*)}) = \mathcal{B}(B \rightarrow K^{(*)}\mu^+\mu^-)/\mathcal{B}(B \rightarrow K^{(*)}e^+e^-)$

- **FCNC  $b \rightarrow s\ell\ell$**
- Rare decay forbidden at the tree level
- Very sensitive to NP contributions in the loops



►  $R(X_c) = \mathcal{B}(B \rightarrow X_c\tau^+\nu_\tau)/\mathcal{B}(B \rightarrow X_c\mu^+\nu_\mu)$ ,  $X_c = D, D^*$  or  $J/\psi$

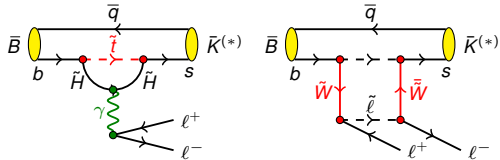
- **Tree level  $b \rightarrow c\tau\nu_\tau$**
- Abundant semileptonic decay
- Very well known in SM
- Possible NP coupling mainly to the 3rd family



# In this talk: two front LFU tests

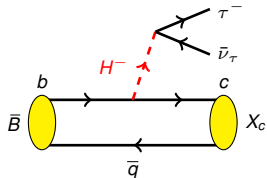
►  $R(K^{(*)}) = \mathcal{B}(B \rightarrow K^{(*)}\mu^+\mu^-)/\mathcal{B}(B \rightarrow K^{(*)}e^+e^-)$

- **FCNC**  $b \rightarrow s\ell\ell$
- Rare decay forbidden at the tree level
- Very sensitive to NP contributions in the loops



►  $R(X_c) = \mathcal{B}(B \rightarrow X_c\tau^+\nu_\tau)/\mathcal{B}(B \rightarrow X_c\mu^+\nu_\mu)$ ,  $X_c = D, D^*$  or  $J/\psi$

- **Tree level**  $b \rightarrow c\tau\nu_\tau$
- Abundant semileptonic decay
- Very well known in SM
- Possible NP coupling mainly to the 3rd family



# LHCb: general-purpose detector in the forward region at the LHC

[Int. J. Mod. Phys. A 30, 1530022 (2015)]

LHCb is a forward spectrometer installed on the LHC  
with a **broad physics program** continually expanding:

- CKM and CP violation in  $b$  and  $c$  hadrons
- Rare decays of  $b$  and  $c$  hadrons
- Heavy quark production
- Spectroscopy including tetraquarks, pentaquarks, ...
- Kaon physics
- Electroweak, QCD, exotica, ...
- Higgs and top
- Heavy ion physics (p-Pb, Pb-Pb), fixed-target collisions (He, Ne, Ar).

Examples of publications, well beyond  $b$ -physics:

[Search for Majorana neutrinos in  $B^- \rightarrow \pi \mu^+ \mu^+$  decays, PRL 2014],

[Search for dark photons produced in 13 TeV  $p\bar{p}$  collision, PRL 2018],

[Measurement of forward top pair production in the dilepton channel in  $p\bar{p}$  collisions at  $\sqrt{s} = 13$  TeV, 1803.05188],

[Measurements of long-range near-side angular correlations in  $\sqrt{s_{NN}} = 5$  TeV proton-lead collisions in the forward region, PLB 2016],

[Limits on neutral Higgs boson production in the forward region in  $p\bar{p}$  collisions at  $\sqrt{s} = 7$  TeV, JHEP 2013]

# The LHCb detector

[Int. J. Mod. Phys. A 30, 1530022 (2015)]

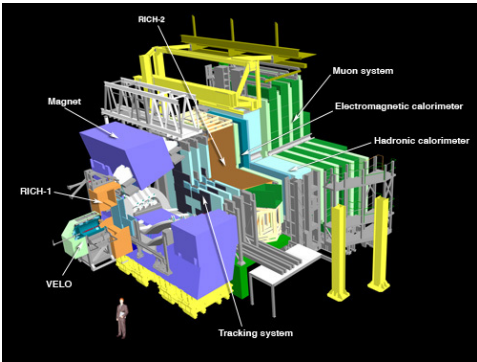
## ► Advantages:

- Excellent vertexing, tracking and PID
- Trigger also on low momentum hadrons
- Enormous data sample from LHC high  $b\bar{b}$  cross section
- All type of b-hadrons, including  $B_c^+$  and  $\Lambda_b$

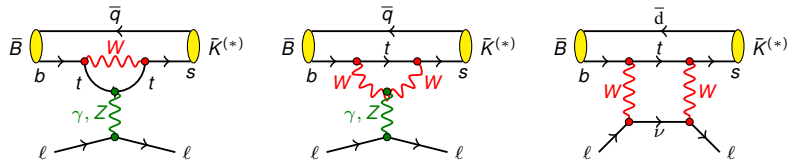
## ► Challenges:

- Missing neutrinos → unconstrained kinematics
- High track multiplicity → significant amount of background
- High particle momenta → significant Bremsstrahlung for electrons

In this talk: ONLY Run 1 data,  $3 \text{ fb}^{-1}$ , 2011(12),  $\sqrt{s} = 7(8) \text{ TeV}$



# 1. LFU tests with $b \rightarrow s\ell\ell$ : $R_K, R_{K^{*0}}$



# Test of LFU with $B^+ \rightarrow K^+\ell^+\ell^-$

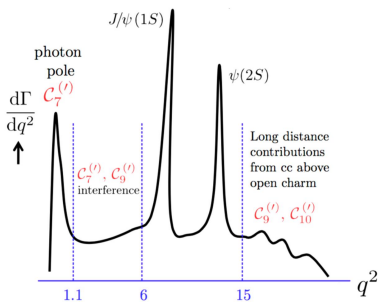
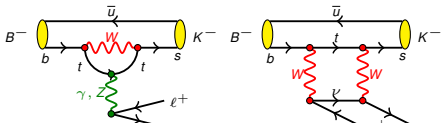
[PRL, 113, 151601 (2014)]

- In the SM:  
 $R_K \equiv \frac{\mathcal{B}(B^+ \rightarrow K^+\mu^+\mu^-)}{\mathcal{B}(B^+ \rightarrow K^+e^+e^-)} = 1 \pm \mathcal{O}(10^{-3})$

[e.g. PRL 112, 149902 (2014)]

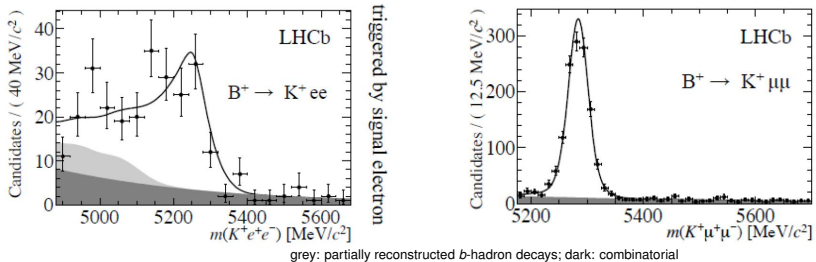
- In 2014, LHCb measured  $R_K$  for  
 $q^2 = m_{\ell\ell}^2 \in [1, 6] \text{ GeV}^2/c^4$   
 (avoid resonance regions)
- Extremely challenging due to  
 differences in the way  $\mu$  and  $e$  interact  
 with detector: Bremsstrahlung and  
 trigger
- Signal extracted via invariant mass fits
- Measure using double ratio to  
 minimize uncertainties:

$$R_K = \frac{\mathcal{B}(B^+ \rightarrow K^+\mu^+\mu^-)}{\mathcal{B}(B^+ \rightarrow K^+J/\psi(\rightarrow \mu^+\mu^-))} / \frac{\mathcal{B}(B^+ \rightarrow K^+e^+e^-)}{\mathcal{B}(B^+ \rightarrow K^+J/\psi(\rightarrow e^+e^-))}$$

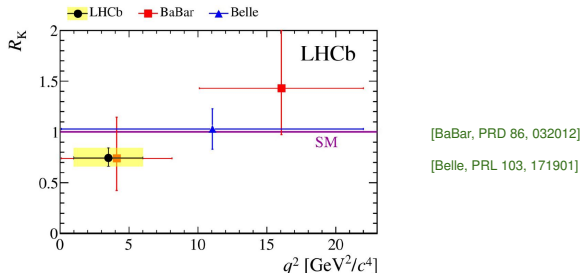


# Test of LFU with $B^+ \rightarrow K^+ \ell^+ \ell^-$

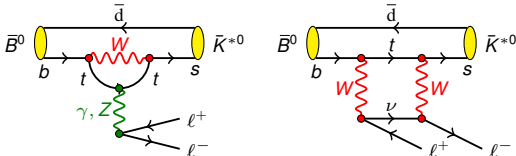
[PRL, 113, 151601 (2014)]



$$R_K(\text{LHCb}, 1 < q^2 < 6 \text{ GeV}^2/c^4) = 0.745^{+0.090}_{-0.074} \pm 0.036 \text{ (2.6}\sigma\text{ below SM)}$$



$$R_{K^{*0}} = \frac{\mathcal{B}(B^0 \rightarrow K^{*0} \mu^+ \mu^-)}{\mathcal{B}(B^0 \rightarrow K^{*0} e^+ e^-)}$$



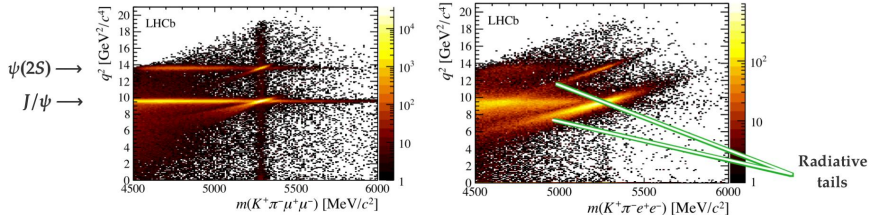
- Similar to  $R_K$ .  $K^{*0}$  reconstructed into  $K^+ \pi^-$
- Measured in two  $q^2$  bins  $[0.045 - 1.1]$  (low) and  $[1.1 - 6] \text{ GeV}^2/c^4$  (central)
- Double ratio to minimize uncertainties:

$$R_{K^{*0}} = \frac{\mathcal{B}(B^0 \rightarrow K^{*0} \mu^+ \mu^-)}{\mathcal{B}(B^0 \rightarrow K^{*0} J/\psi (\rightarrow \mu^+ \mu^-))} / \frac{\mathcal{B}(B^0 \rightarrow K^{*0} e^+ e^-)}{\mathcal{B}(B^0 \rightarrow K^{*0} J/\psi (\rightarrow e^+ e^-))}$$

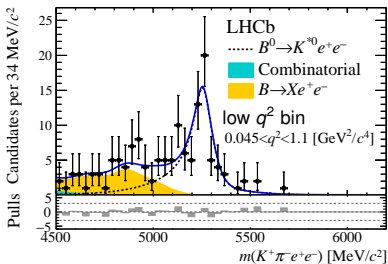
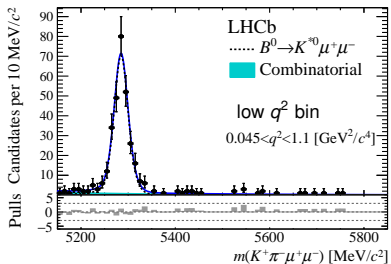
- Challenges are again trigger and Bremsstrahlung due to differences between  $\mu$  and  $e$

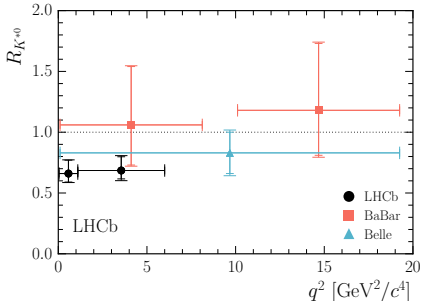
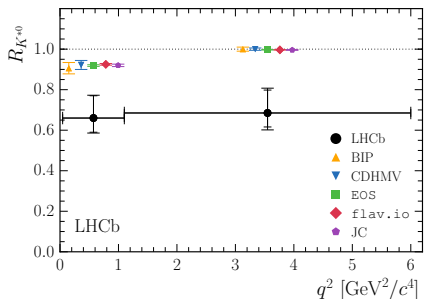
# Test of LFU with $B^0 \rightarrow K^{*0} \ell^+ \ell^-$

[JHEP 08 (2017) 055]



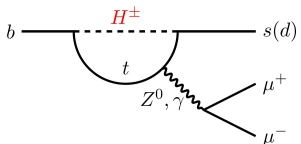
- Fit  $K^+ \pi^- \ell^+ \ell^-$  mass in low and central  $q^2$  bins
- Simultaneous fit to  $J/\psi$  and non-resonant channels



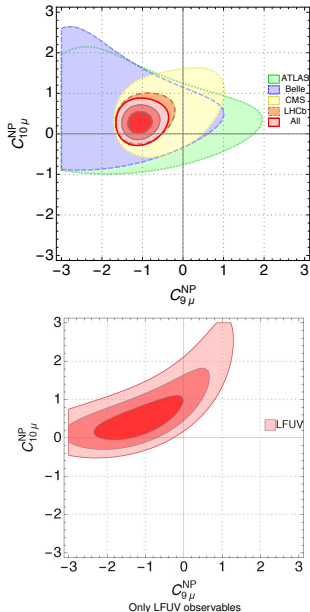


- Lower bin:  $R_{K^{*0}} = 0.66^{+0.11}_{-0.07}(\text{stat}) \pm 0.03(\text{syst})$   **$2.1 - 2.3\sigma$  below SM**
- Central bin:  $R_{K^{*0}} = 0.69^{+0.11}_{-0.07}(\text{stat}) \pm 0.05(\text{syst})$   **$2.4 - 2.5\sigma$  below SM**
- Combining  $R_K$  and  $R_{K^{*0}}$ : see e.g. [Capdevila et al., JHEP 1801 (2018) 093]  
**"LFU violation favored at  $3.3\sigma$  wrt LFU"**

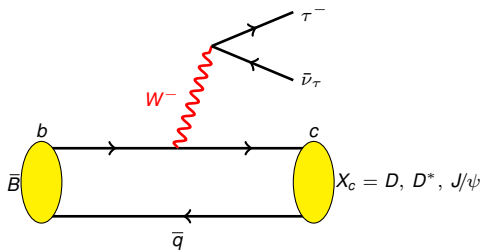
# Neutral current anomalies $b \rightarrow s\ell\ell$



- Not only  $R_K$  and  $R_{K^{*0}}$ , several other measurements involving  $b \rightarrow s\ell\ell$ , ( $\ell = \mu, e$ ) deviate from their SM expectation ( $2 - 3\sigma$ ):  
BR of  $B^0 \rightarrow K^* \mu^+ \mu^-$ ,  $B_s^0 \rightarrow \phi \mu^+ \mu^-$ ,  
 $\Lambda_b \rightarrow \Lambda^0 \mu^+ \mu^-$ ,  $P'_5$
- The combined effect of these “small” deviations point towards the same direction:  
 $C_{9\mu}^{\text{NP}} = -1$ , implying **violation of the leptonic universality**  $\mu \neq e$ .  
Significance of global fits  $\sim 5\sigma$  (top plot);  
 $> 3.3\sigma$  if only LFUV observables are considered (bottom) [Capdevila et al., JHEP 1801 (2018) 093]
- Deficit of muons? Theoretical uncertainties or experimental?



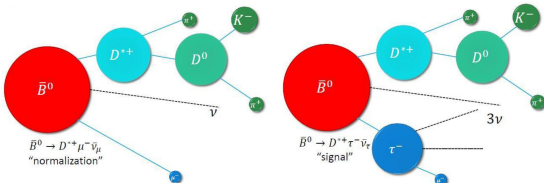
## 2. LFU tests with $b \rightarrow c\tau\nu_\tau$ : $R(D), R(D^*), R(J/\psi)$



# $R(D^*)$ muonic ( $\tau^+ \rightarrow \mu^+ \nu_\mu \bar{\nu}_\tau$ ) [PRL 115 (2015) 112001]

$$R(D^*) = \frac{\mathcal{B}(B^0 \rightarrow D^{*-} \tau^+ \nu_\tau)}{\mathcal{B}(B^0 \rightarrow D^{*-} \mu^+ \nu_\mu)}$$

with  $\tau^+ \rightarrow \mu^+ \nu_\mu \bar{\nu}_\tau$



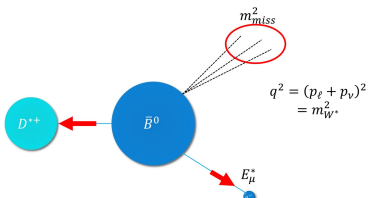
- Precise SM prediction:  $R(D^*) = 0.252 \pm 0.003$

[S.Fajfer et al., PRD 85(2012) 094025]

- Normalization mode with the same final state
- $\mathcal{B}(\tau^+ \rightarrow \mu^+ \nu_\mu \bar{\nu}_\tau) = (17.39 \pm 0.04)\%$
- Neutrinos: no narrow peak to fit
- Separate  $\tau$  and  $\mu$  via a 3D binned template fit, in the  $B$  rest frame, on:

- 1  $m_{\text{miss}}^2 = (p_B^\mu - p_{D^*}^\mu - p_\mu^\mu)^2$
- 2  $E_\mu^*$
- 3  $q^2 = (p_B^\mu - p_{D^*}^\mu)^2$

- Background and signal shapes extracted from control samples and simulations validated against data



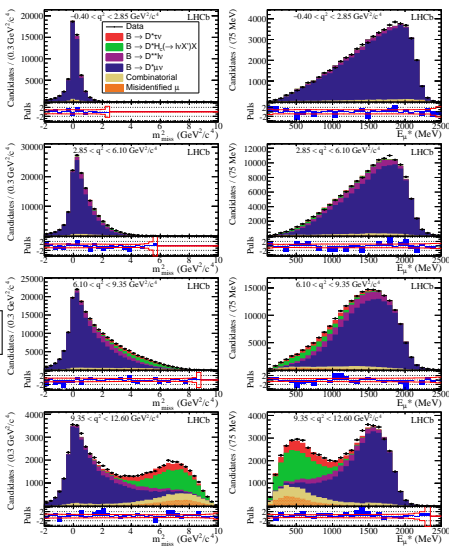
# $R(D^*)$ muonic ( $\tau^+ \rightarrow \mu^+ \nu_\mu \bar{\nu}_\tau$ ) [PRL 115 (2015) 112001]

- Signal more visible in the high  $q^2$  bins (red)
- Backgrounds: feed-down from excited  $D$  states, double charm  $DD$  where one  $D$  decays semileptonically, combinatorial, muon mis-ID

$$R(D^*) = 0.336 \pm 0.027(\text{stat}) \pm 0.030(\text{syst})$$

2.1 $\sigma$  above SM

- Dominant systematics: size of simulation sample → will be improved in the next iteration

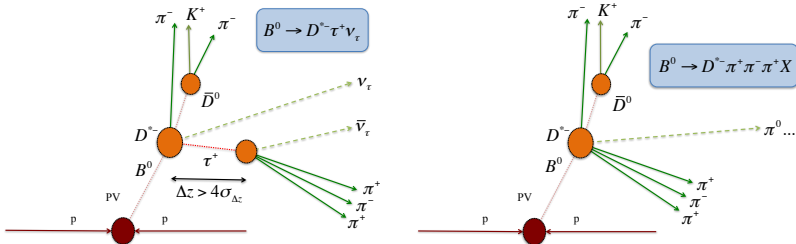


# $R(D^*)$ hadronic ( $\tau \rightarrow 3\pi\nu_\tau$ ) [PRL 120, 171802 2018], [PRD 97,072013 2018]

$$R(D^*) = \mathcal{K}(D^*) \times \frac{\mathcal{B}(B^0 \rightarrow D^{*-} 3\pi)}{\mathcal{B}(B^0 \rightarrow D^{*-} \mu^+ \nu_\mu)}$$

with  $\mathcal{K}(D^*) = \frac{\mathcal{B}(B^0 \rightarrow D^{*-} \tau^+ \nu_\tau)}{\mathcal{B}(B^0 \rightarrow D^{*-} 3\pi)}, \tau^+ \rightarrow 3\pi(\pi^0)\nu_\tau$

- Signal and normalization modes chosen to have the same final state
- $\mathcal{B}(\tau \rightarrow 3\pi(\pi^0)\nu_\tau) \simeq 13.9\%$  (was  $\sim 17\%$  for the muonic case)
- No charged lepton in final state: zero bkg from  $B^0 \rightarrow D^{*-} \mu^+ \nu_\mu$  and good  $\tau$  vertex reconstruction but large hadronic bkg:  $B \rightarrow D^* 3\pi X$  (BR  $\sim 100 \times$  signal),  $B \rightarrow D^* D_s X$  (BR  $\sim 10 \times$  signal)
- Main bkg ( $B \rightarrow D^* 3\pi X$ ) suppressed by requiring the  $\tau$  vertex to be downstream wrt  $B$  vertex along beam direction
- BDT used to suppressed the remaining background (mainly  $B \rightarrow D^* D_s X$ )



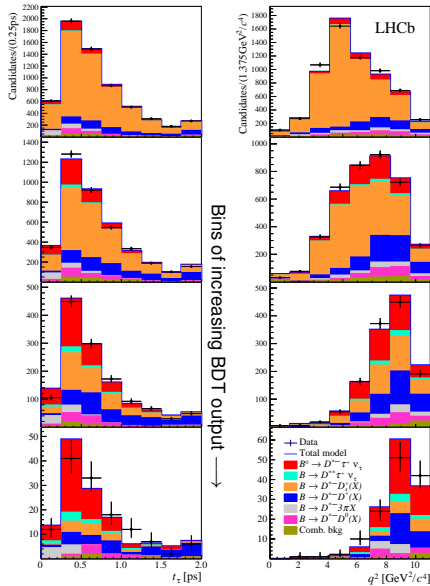
# $R(D^*)$ hadronic ( $\tau \rightarrow 3\pi\nu_\tau$ ) [PRL 120, 171802 2018], [PRD 97,072013 2018]

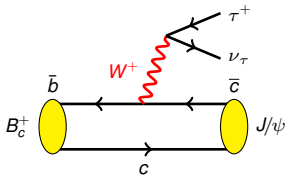
- $N(B^0 \rightarrow D^{*-} \tau^+ \nu_\tau)$  from 3D binned fit on BDT output,  $\tau$  decay time and  $q^2$
- Templates extracted from simulation and data control samples
- $N(B^0 \rightarrow D^{*-} \tau^+ \nu_\tau) = 1300 \pm 85$

$$R(D^*) = 0.291 \pm 0.019(\text{stat}) \\ \pm 0.026(\text{syst}) \pm 0.013(\text{ext})$$

1.0 $\sigma$  above SM

- Dominant systematics: size of simulation samples





- Generalization of  $R(D^*)$  to  $B_c^+$

$$R(J/\psi) = \frac{\mathcal{B}(B_c^+ \rightarrow J/\psi \tau^+ \nu_\tau)}{\mathcal{B}(B_c^+ \rightarrow J/\psi \mu^+ \nu_\mu)}$$

- $B_c^+$  decay form factors unconstrained experimentally: theoretical prediction not yet precise  $R^{\text{theo}}(J/\psi) \in [0.25, 0.28]$

[PLB452 (1999) 120, arXiv:0211021, PRD73 (2006) 054024, PRD74 (2006) 074008]

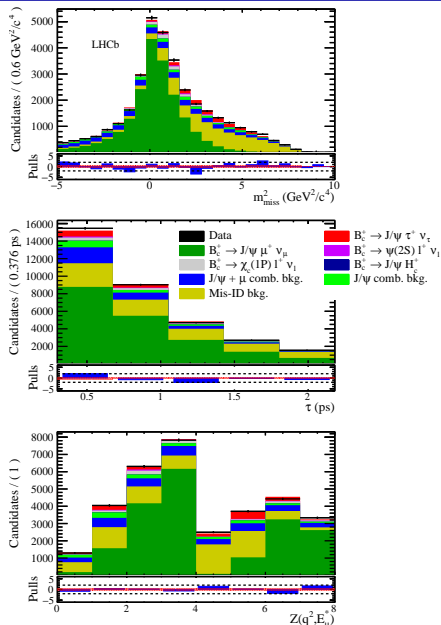
- Reconstruct signal with  $\tau^+ \rightarrow \mu^+ \nu_\mu \bar{\nu}_\tau$
- Like in  $R(D^*)$ , use  $m_{\text{miss}}^2$ ,  $E_\mu^*$  and  $q^2$ . Add information from  $B_c^+$  decay time

- 3D template binned fit
- Shapes of various components are represented by a template distribution derived from control samples or simulations validated against data
- Main background is  $b \rightarrow J/\psi + \text{mis-ID hadron}$
- First evidence for the decay  $B_c^+ \rightarrow J/\psi \tau^+ \nu_\tau$  ( $3\sigma$ )

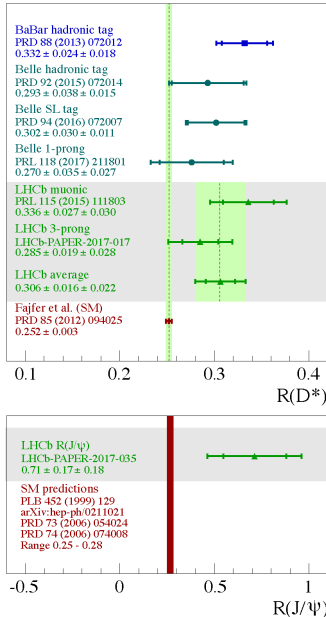
$$R(J/\psi) = 0.71 \pm 0.17 \pm 0.18$$

About  $2\sigma$  above SM

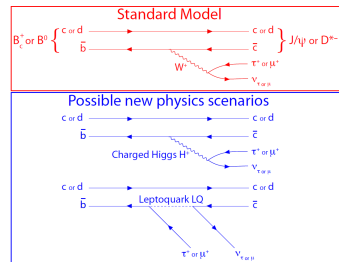
- Main systematics: form factor and size of simulation sample



# $R(D^*)$ and $R(J/\psi)$ summary



3 experiments, 7 measurements,  
different analysis techniques:  
**ALL  $R(D^*)$  and  $R(J/\psi)$  measurements lie ABOVE the SM expectations!**



# $R(D^*)$ and $R(D)$ summary

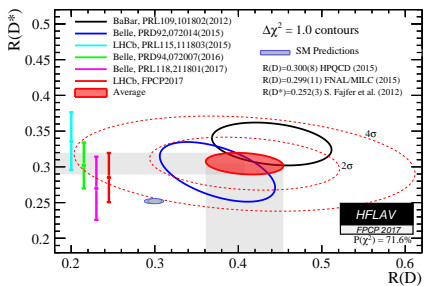
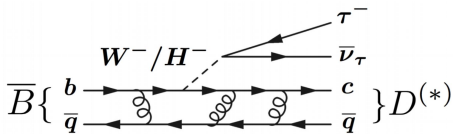
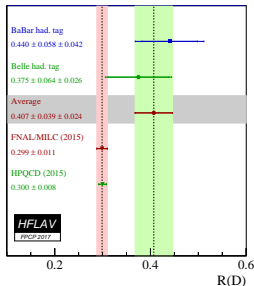
- Similarly to  $R(D^*)$ , the ratio is defined for  $D^-$  mesons:

$$R(D) = \frac{\mathcal{B}(B^0 \rightarrow D^- \tau^+ \nu_\tau)}{\mathcal{B}(B^0 \rightarrow D^- \ell^+ \nu_\ell)}$$

and has been measured by Belle and BaBar

- Theoretical predictions:  $R(D) = 0.300 \pm 0.008$ ,

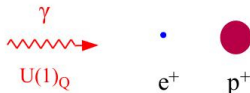
[HPQCD, PRD 92, 054510 (2015)]



- Combination of LHCb, Belle and BaBar:  **$4.1\sigma$  wrt SM!**

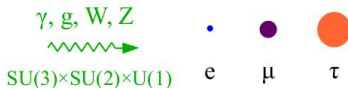
# Before concluding...

Let's go back ~ 100 years, and suppose we can test matter only with long wavelength photons...



These two particles seems to be  
“identical copies” but for their mass ...

That's exactly the same (misleading) argument we use to infer LFU...



These three (families) of particles  
seems to be “identical copies”  
but for their mass ...

The SM quantum numbers of the three families could be an “accidental” low-energy property: the different families may well have a very different behavior at high energies, as signaled by their different mass

# Conclusions and prospects

- ▶ **Exciting time for LFU tests with TWO anomalies:**
  - **Charged current  $b \rightarrow c\tau\nu$ ,  $4.1\sigma$  tension in  $R(D) - R(D^*)$**  when combining BaBar, Belle and LHCb results. Recent  $2\sigma$  discrepancy in the same direction observed by LHCb in  $B_c^+ \rightarrow J/\psi \tau^+ \nu_\tau$
  - **FCNC  $b \rightarrow s\ell\ell$ , notably  $R_K$  and  $R_{K^{*0}}$ .** LFU violation favored at more than  $3\sigma$
- ▶ Measurements presented performed with Run 1  
Many more to come with larger data sets:
  - $b \rightarrow c\tau\nu$ :  $R(D^0)$ ,  $R(D^+)$ ,  $R(D_s^{(*)})$ ,  $R(\Lambda_c^{(*)})$ , ...
  - $b \rightarrow s\ell\ell$ :  $R_\phi$ ,  $R_{pK}$ ,  $R_{K\pi\pi}$ ,  $R_{K_S^0}$ ,  $R_{K^{*+}}$ , ...
  - Spin 0, 1/2, 1 in the final state + angular observables,  $BR(q^2)$ , ...  
→ Would allow to differentiate various NP scenarios
- ▶ LHCb Run 2 (2015-2018)  $\simeq$  Run 1  $\times 3$ .  
Then, Upgrade, Run 3, 4 and plans until 2037!  
Also complementarity and competition from Belle II
- ▶ Exciting work-plan in the coming years, with **crucial interplay between experiment and theory**

# Backups

Page 27 Phenomenology

Page 31  $R_K$

Page 33  $R_{K^{*0}}$

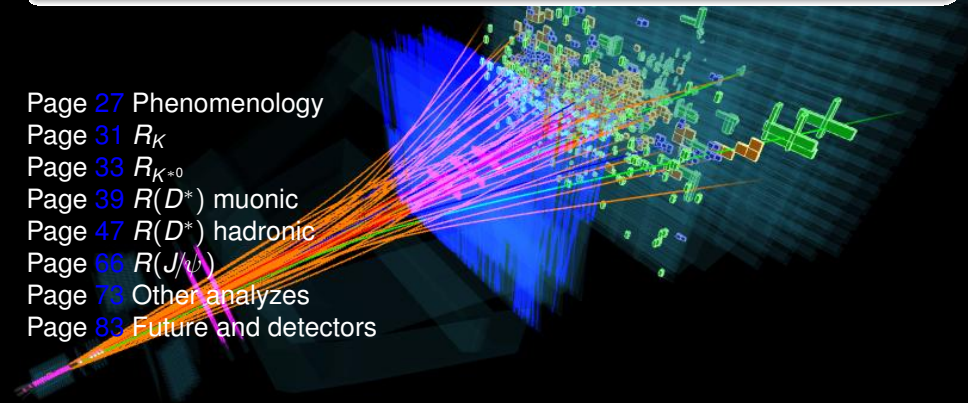
Page 39  $R(D^*)$  muonic

Page 47  $R(D^*)$  hadronic

Page 66  $R(J/\psi)$

Page 73 Other analyzes

Page 83 Future and detectors



# Tantalizing tensions with respect to the SM

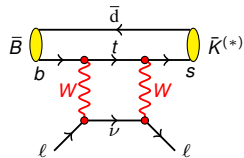
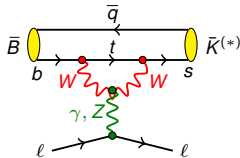
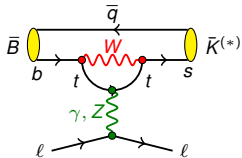
Observable	Tension wrt SM	Limited by
$B \rightarrow D^{(*)}\tau\nu/B \rightarrow D^{(*)}\ell\nu, \ell = \mu, e$	$4.1\sigma$	experiment
$(g-2)_\mu$	$3.6\sigma$	exp. & theo.
$B^0 \rightarrow K^{*0}\mu\mu$ angular dist., BR	$3.4\sigma$	exp. & theo.
$B_s^0 \rightarrow \phi\mu\mu$ BR	$3.0\sigma$	experiment
$2\sigma(W \rightarrow \tau\nu_\tau)/(\sigma(W \rightarrow e\nu_e) + \sigma(W \rightarrow \mu\nu_\mu))$	$2.8\sigma$	experiment
$B^+ \rightarrow K^+\mu\mu/B^+ \rightarrow K^+ee$	$2.6\sigma$	experiment
$B^0 \rightarrow K^{*0}\mu\mu/B^0 \rightarrow K^{*0}ee$	$2.6\sigma$	experiment
$B_c \rightarrow J/\psi\tau\nu/B_c \rightarrow J/\psi\mu\nu$	$2.0\sigma$	exp. & theo.

Many other interesting results exhibit no tension today, but put strong constraints on NP models.

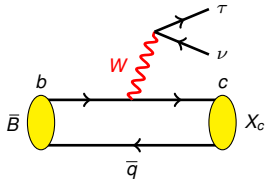
They remain fundamental for future searches, e.g.:  $\gamma$ ,  $B^0$ - $D^0$ - $K^0$ -mixing,  $\phi_s$ ,  $\sin 2\beta$ ,  $B_s^0 \rightarrow \mu\mu$ ,  $B \rightarrow X_s\gamma$ ,  $V_{cb}$ ,  $B \rightarrow \tau\nu$ , CPV in charm, CLVF,  $K \rightarrow \pi\nu\bar{\nu}$ , ...

# Flavor Anomalies

- $b \rightarrow s l \bar{l}$



- $b \rightarrow c \tau \nu_\tau$



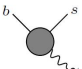
# Effective field theory

Transition  $B \rightarrow f$  described by an effective Hamiltonian  $\langle f | \mathcal{H}_{\text{eff}} | B \rangle$ , with

$$\mathcal{H}_{\text{eff}} = -\frac{4G_F}{\sqrt{2}} V_{tb} V_{tq}^* \sum_i \left( \underbrace{C_i \mathcal{O}_i}_{\text{Left-handed}} + \underbrace{C'_i \mathcal{O}'_i}_{\text{Right-handed}} \right)$$

Computed by splitting into:

- $C_i$  (Wilson coefficients): short distance (perturbative) effective couplings, can be computed in terms of fundamental couplings of the SM and beyond
- $\langle f | \mathcal{O}_i | B \rangle$ : long distance (non perturbative), computed using QCD at low energy or extracted by phenomenological analysis.  $\mathcal{O}_i$  are local operators:

$\mathcal{O}_7^{(\prime)}$ photon penguin	$b \rightarrow s\gamma$	$B \rightarrow \mu\mu$	$b \rightarrow s\ell\ell$
	✓		✓
$\mathcal{O}_9^{(\prime)}$ vector coupling			✓
$\mathcal{O}_{10}^{(\prime)}$ axialvector coupling		✓	✓
$\mathcal{O}_{S,P}^{(\prime)}$ (pseudo)scalar penguin		✓	

# Fundamental parameters of the Standard Model

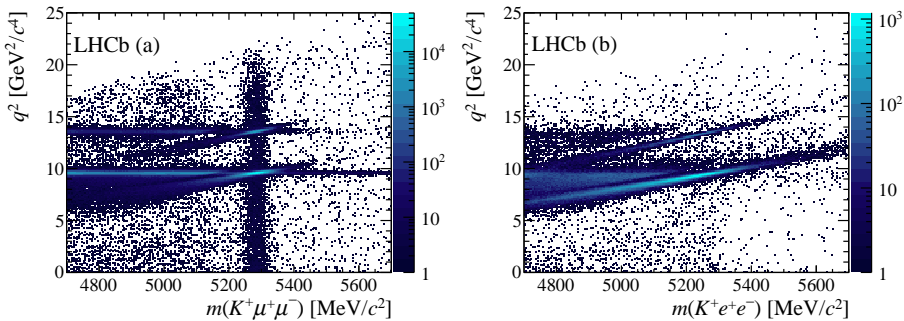
The 28 parameters of the Standard Model are:

- the 3 coupling constant associated to  $SU(2)_L \times U(1)_Y$  and  $SU(3)_c$ ,
- the 2 Higgs field potential parameters  $\mu$  and  $\lambda$ ,
- the six quark masses and the six lepton masses,
- the four CKM parameters
- the six MNS parameters
- the possible QCD CP violating phase  $\theta_{\text{QCD}}$ .

# $R_K, R_{K^{*0}}$

# Test of LFU with $B^+ \rightarrow K^+\ell^+\ell^-$

[PRL, 113, 151601 (2014)]



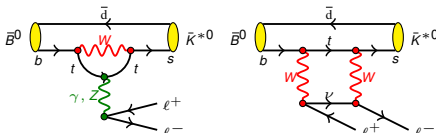
$$R_K(\text{LHCb}, 1 < q^2 < 6 \text{ GeV}^2/c^4) = 0.745^{+0.090}_{-0.074} \pm 0.036 \quad (\text{2.6}\sigma \text{ from SM})$$

The dominant sources of systematic uncertainty are due to the parametrization of the  $B^+ \rightarrow J/\psi K e^+ e^-$  mass distribution and the estimate of the trigger efficiencies that both contribute 3% to the value of  $R_K$

# Test of LFU with $B^0 \rightarrow K^{*0} \ell^+ \ell^-$

[JHEP 08 (2017) 055]

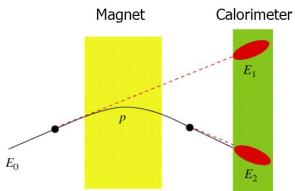
$$R_{K^{*0}} = \frac{\mathcal{B}(B^0 \rightarrow K^{*0} \mu^+ \mu^-)}{\mathcal{B}(B^0 \rightarrow K^{*0} e^+ e^-)}$$

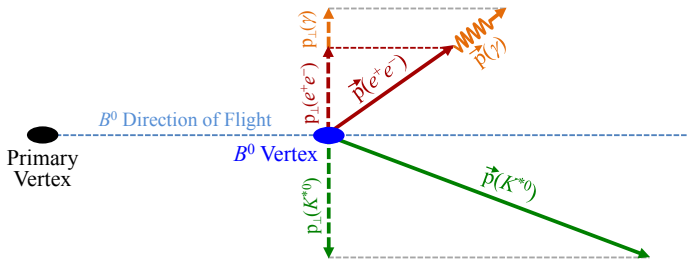


- Similar to  $R_K$
- Measured in two  $q^2$  bins  $[0.045 - 1.1]$  and  $[1.1 - 6] \text{ GeV}^2/c^4$ , with  $K^{*0} \rightarrow K^+ \pi^-$
- Double ratio to minimize uncertainties:

$$R_{K^{*0}} = \frac{\mathcal{B}(B^0 \rightarrow K^{*0} \mu^+ \mu^-)}{\mathcal{B}(B^0 \rightarrow K^{*0} J/\psi (\rightarrow \mu^+ \mu^-))} / \frac{\mathcal{B}(B^0 \rightarrow K^{*0} e^+ e^-)}{\mathcal{B}(B^0 \rightarrow K^{*0} J/\psi (\rightarrow e^+ e^-))}$$

- Challenges are again trigger and Bremsstrahlung due to differences between  $\mu$  and  $e$
- Electrons  $\rightarrow$  larger Bremsstrahlung  $\rightarrow$  degraded momentum and mass resolution
- Recovery momentum procedure: extrapolation of the electron track upstream of the magnet and addition of calorimeter cluster to the electron momentum

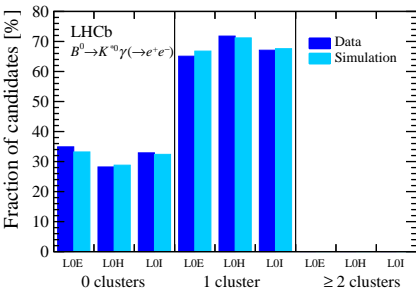
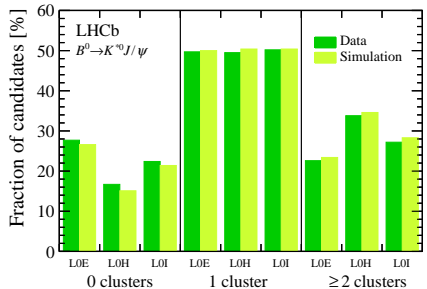




Sketch of the topology of a  $B^0 \rightarrow K^{*0} e^+ e^-$  decay. The transverse momentum lost via bremsstrahlung is evaluated as the difference between the  $p_T$  of the  $K^{*0}$  meson and that of the dielectron system, where both are calculated with respect to the  $B^0$  meson direction of flight. Bremsstrahlung photons that are not recovered by the reconstruction are assumed to follow the dielectron momentum direction.

# Test of LFU with $B^0 \rightarrow K^{*0} \ell^+ \ell^-$

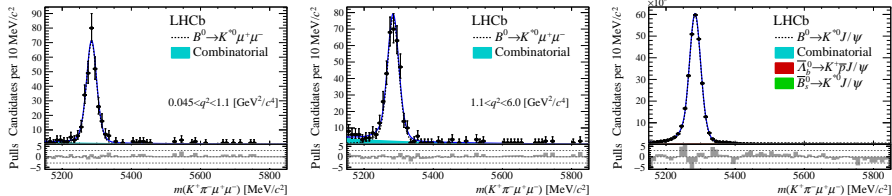
[JHEP 08 (2017) 055]



Fraction of (left)  $B^0 \rightarrow K^{*0} J/\psi (\rightarrow e^+ e^-)$  and (right)  $B^0 \rightarrow K^{*0} \gamma (\rightarrow e^+ e^-)$  candidates (in percent) with zero, one, and two or more recovered clusters per trigger category. The numbers are from (darker colour) data and (lighter colour) simulation. Due to the very low opening angle of the two electrons in  $B^0 \rightarrow K^{*0} \gamma (\rightarrow e^+ e^-)$  decays, the bremsstrahlung photon energy deposits overlap and only one bremsstrahlung cluster at most is resolved.

# Test of LFU with $B^0 \rightarrow K^{*0} \ell^+ \ell^-$

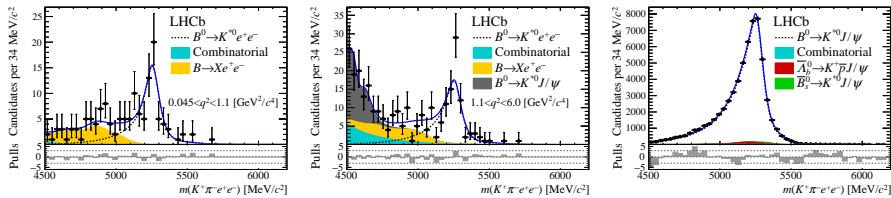
[JHEP 08 (2017) 055]



Fit to the  $m(K^+\pi^-\mu^+\mu^-)$  invariant mass of (top)  $B^0 \rightarrow K^{*0} \mu^+ \mu^-$  in the low- and central- $q^2$  bins and (bottom)  $B^0 \rightarrow K^{*0} J/\psi (\rightarrow \mu^+ \mu^-)$  candidates. The dashed line is the signal PDF, the shaded shapes are the background PDFs and the solid line is the total PDF. The fit residuals normalised to the data uncertainty are shown at the bottom of each distribution.

# Test of LFU with $B^0 \rightarrow K^{*0} \ell^+ \ell^-$

[JHEP 08 (2017) 055]



Fit to the  $m(K^+\pi^-e^+e^-)$  invariant mass of (top)  $B^0 \rightarrow K^{*0} e^+ e^-$  in the low- and central- $q^2$  bins and (bottom)  $B^0 \rightarrow K^{*0} J/\psi (\rightarrow e^+ e^-)$  candidates. The dashed line is the signal PDF, the shaded shapes are the background PDFs and the solid line is the total PDF. The fit residuals normalised to the data uncertainty are shown at the bottom of each distribution.

$B \rightarrow X(\rightarrow Y K^{*0}) e^+ e^-$ : (the decay product  $Y$  is not reconstructed), is obtained from simulation using a sample that includes decays of higher kaon resonances,  $X$ , such as  $K_1^+(1270)$  and  $K_2^{*+}(1430)$ .

Systematic uncertainties on the  $R_{K^{*0}}$  ratio for the three trigger categories separately (in percent). The total uncertainty is the sum in quadrature of all the contributions.

Trigger category	$\Delta R_{K^{*0}} / R_{K^{*0}} [\%]$					
	low- $q^2$			central- $q^2$		
	L0E	L0H	L0I	L0E	L0H	L0I
Corrections to simulation	2.5	4.8	3.9	2.2	4.2	3.4
Trigger	0.1	1.2	0.1	0.2	0.8	0.2
PID	0.2	0.4	0.3	0.2	1.0	0.5
Kinematic selection	2.1	2.1	2.1	2.1	2.1	2.1
Residual background	—	—	—	5.0	5.0	5.0
Mass fits	1.4	2.1	2.5	2.0	0.9	1.0
Bin migration	1.0	1.0	1.0	1.6	1.6	1.6
$R_{J/\psi}$ ratio	1.6	1.4	1.7	0.7	2.1	0.7
Total	4.0	6.1	5.5	6.4	7.5	6.7

L0E: electron trigger

L0H: hadron trigger

L0I: trigger independent of the signal

Largest systematics from trigger and mass modelling

$R(D^*)$  muonic ( $\tau^+ \rightarrow \mu^+ \nu_\mu \bar{\nu}_\tau$

# Full angular distribution in $B \rightarrow D^*(\rightarrow D\pi)\ell\bar{\nu}_\ell$

[D. Bećirević, S. Fajfer, I. Nišandžić, A. Tayduganov, arXiv:1602.03030]

The full angular distribution is given by

$$\frac{d^4\Gamma}{dq^2 d\cos\theta_\ell d\cos\theta_D d\chi} = \frac{3G_F^2 |V_{cb}|^2}{256(2\pi)^4 m_B^3} q^2 \left(1 - \frac{m_\ell^2}{q^2}\right)^2 \sqrt{\lambda_D^*(q^2)} \times B(D^* \rightarrow D\pi) \times \left\{ \begin{aligned} & [|H_+|^2 + |H_-|^2] \left(1 + \cos^2\theta_\ell + \frac{m_\ell^2}{q^2} \sin^2\theta_\ell\right) \sin^2\theta_D + 2[|H_+|^2 - |H_-|^2] \cos\theta_\ell \sin^2\theta_D \\ & + 4|H_0|^2 \left(\sin^2\theta_\ell + \frac{m_\ell^2}{q^2} \cos^2\theta_\ell\right) \cos^2\theta_D + 4|H_t|^2 \frac{m_\ell^2}{q^2} \cos^2\theta_D \\ & - 2\beta_\ell^2 (\Re[H_+ H_-^*] \cos 2\chi + \Im[H_+ H_-^*] \sin 2\chi) \sin^2\theta_\ell \sin^2\theta_D \\ & - \beta_\ell^2 \left( \Re[H_+ H_0^* + H_- H_0^*] \cos\chi + \Im[H_+ H_0^* - H_- H_0^*] \sin\chi \right) \sin 2\theta_\ell \sin 2\theta_D \\ & - 2\Re \left[ H_+ H_0^* - H_- H_0^* - \frac{m_\ell^2}{q^2} (H_+ H_t^* + H_- H_t^*) \right] \cos\chi \sin\theta_\ell \sin 2\theta_D \\ & - 2\Im \left[ H_+ H_0^* + H_- H_0^* - \frac{m_\ell^2}{q^2} (H_+ H_t^* - H_- H_t^*) \right] \sin\chi \sin\theta_\ell \sin 2\theta_D \\ & + 8\Re[H_0 H_t^*] \frac{m_\ell^2}{q^2} \cos\theta_\ell \cos^2\theta_D \end{aligned} \right\}, \quad \beta_\ell(q^2) = \sqrt{1 - \frac{m_\ell^2}{q^2}}, \quad H(q^2) = \tilde{\varepsilon}^{\mu*} \langle D^*(\varepsilon) | J_\mu | \bar{B} \rangle$$

# $B \rightarrow D^*(\rightarrow D\pi)\ell\bar{\nu}_\ell$ : observables sensitive to NP

[D. Bećirević, S. Fajfer, I. Nišandžić, A. Tayduganov, arXiv:1602.03030]

What can be extracted from the proposed observables:

$d\Gamma/dq^2$	$\left[ H_+ ^2 +  H_- ^2 +  H_0 ^2\right] \left(1 + \frac{m_\ell^2}{2q^2}\right) + \frac{3}{2} \frac{m_\ell^2}{q^2}  H_t ^2$	
$1 - \mathcal{A}_{\lambda_\ell}$	$ H_+ ^2 +  H_- ^2 +  H_0 ^2 + 3 H_t ^2$	
$\mathcal{A}_{FB}$	$ H_+ ^2 -  H_- ^2 + 2 \frac{m_\ell^2}{q^2} \Re[H_0 H_t^*]$	
$R_{L,T}$	$ H_+ ^2 +  H_- ^2$	
$A_5$	$ H_+ ^2 -  H_- ^2$	
$C_\chi$	$\Re[H_+ H_-^*]$	
$S_\chi$	$\Im[H_+ H_-^*]$	(=0 in the SM)
$A_8$	$\Im[(H_+ + H_-)H_0^* - \frac{m_\ell^2}{q^2}(H_+ - H_-)H_t^*]$	(=0 in the SM)
$A_9$	$\Re[(H_+ - H_-)H_0^* - \frac{m_\ell^2}{q^2}(H_+ + H_-)H_t^*]$	
$A_{10}$	$\Im[(H_+ - H_-)H_0^*]$	(=0 in the SM)
$A_{11}$	$\Re[(H_+ + H_-)H_0^*]$	

# Best discriminating variable to NP

$$H_{\text{eff}} = \frac{G_F}{\sqrt{2}} V_{cb} [(1 + g_V) \bar{c} \gamma_\mu b + (-1 + g_A) \bar{c} \gamma_\mu \gamma_5 b + g_S i \partial_\mu (\bar{c} b) + g_P i \partial_\mu (\bar{c} \gamma_5 b) \\ + g_T i \partial_\nu (\bar{c} i \sigma_{\mu\nu} b)] (\bar{\ell} \gamma^\mu (1 - \gamma_5) \nu_\ell)$$

[D. Bećirević, S. Fajfer, I. Nišandžić, A. Tayduganov, arXiv:1602.03030]

$\times$ : “not sensitive”  
 $\star\star\star$ : “maximally sensitive”

Quantity	$g_V$	$g_A$	$g_S$	$g_P$	$g_T$
$\mathcal{A}_{FB}^D$	$\times$	—	$\star\star\star$	—	$\star$
$\mathcal{A}_{\lambda_T}^D$	$\times$	—	$\star\star\star$	—	$\star\star$
$\mathcal{A}_{FB}^{D*}$	$\star$	$\star\star\star$	—	$\star\star\star$	$\star$
$\mathcal{A}_{\lambda_T}^{D*}$	$\times$	$\times$	—	$\star\star$	$\star$
$R_{L,T}$	$\times$	$\times$	—	$\star\star$	$\star\star$
$A_5$	$\star\star$	$\star\star$	—	$\star$	$\star\star\star$
$C_x$	$\star$	$\times$	—	$\star\star$	$\star\star$
$S_x$	$\star\star\star$	$\star\star\star$	—	$\times$	$\star\star\star$
$A_8$	$\star\star$	$\star\star$	—	$\star\star$	$\star\star\star$
$A_9$	$\star$	$\star$	—	$\star\star$	$\star\star$
$A_{10}$	$\star\star$	$\star\star$	—	$\times$	$\star\star$
$A_{11}$	$\times$	$\times$	—	$\star\star$	$\star\star$

# $\tau$ lepton Branching Ratios [PDG 2018]

Mode	BR (%)
$\tau^- \rightarrow \pi^- \pi^0 \nu_\tau$	$25.49 \pm 0.09$
$\tau^- \rightarrow e^- \bar{\nu}_e \nu_\tau$	$17.82 \pm 0.04$
$\tau^- \rightarrow \mu^- \bar{\nu}_\mu \nu_\tau$	$17.39 \pm 0.04$
$\tau^- \rightarrow \pi^- \nu_\tau$	$10.82 \pm 0.05$
$\tau^- \rightarrow \pi^- \pi^+ \pi^- \nu_\tau$	$9.31 \pm 0.05$
$\tau^- \rightarrow \pi^- \pi^+ \pi^- \pi^0 \nu_\tau$	$4.62 \pm 0.05$

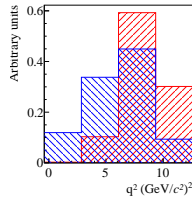
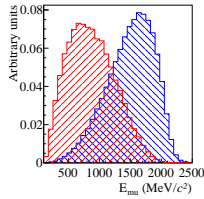
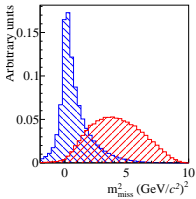
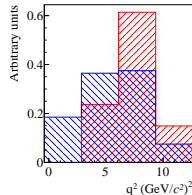
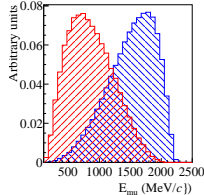
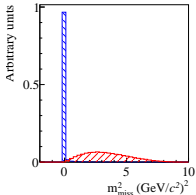
Problem of missing neutrino: no analytical solution for  $p_B$ .

Approximate  $B$  momentum  $p_B^z = \frac{m_B}{m_{D\mu}} p_{D\mu}^z$ .

$m_B$  is the known  $B$  mass,  $m_{D\mu}$  is the reconstructed one.

This leads to  $\sim 18\%$  resolution on  $q^2$ ,  $m_{\text{miss}}^2$  and  $E_\mu^*$ , enough to preserve the discriminating feature of the original variables.

# $R(D^*)$ muonic ( $\tau^+ \rightarrow \mu^+ \nu_\mu \bar{\nu}_\tau$ ) [PRL 115 (2015) 112001]



	$D^* \tau \nu_\tau$	$D^* \mu \nu_\mu$
$m_{\text{miss}}^2$	> 0	$\simeq 0$
$E_\mu^*$	softer	harder
$q^2$	$> m_\tau^2$	$> 0$

Signal(red) and normalization mode (blue) using truth(top) and reconstructed(bottom) quantities

In the  $B$  rest frame:

- $m_{\text{miss}}^2 = (p_B^\mu - p_{D^*}^\mu - p_\mu^\mu)^2$  : missing mass squared
- $E_\mu^*$  : muon energy
- $q^2 = (p_B^\mu - p_{D^*}^\mu)^2$  : squared of the 4-mom transferred to the lepton system

Model uncertainties	Absolute size ( $\times 10^{-2}$ )
Simulated sample size	2.0
Misidentified $\mu$ template shape	1.6
$\bar{B}^0 \rightarrow D^{*+}(\tau^-/\mu^-)\bar{\nu}$ form factors	0.6
$\bar{B} \rightarrow D^{*+}H_c(\rightarrow \mu\nu X')X$ shape corrections	0.5
$\mathcal{B}(\bar{B} \rightarrow D^{**}\tau^-\bar{\nu}_\tau)/\mathcal{B}(\bar{B} \rightarrow D^{**}\mu^-\bar{\nu}_\mu)$	0.5
$\bar{B} \rightarrow D^{**}(\rightarrow D^*\pi\pi)\mu\nu$ shape corrections	0.4
Corrections to simulation	0.4
Combinatorial background shape	0.3
$\bar{B} \rightarrow D^{**}(\rightarrow D^{*+}\pi)\mu^-\bar{\nu}_\mu$ form factors	0.3
$\bar{B} \rightarrow D^{*+}(D_s \rightarrow \tau\nu)X$ fraction	0.1
<b>Total model uncertainty</b>	<b>2.8</b>
Normalization uncertainties	Absolute size ( $\times 10^{-2}$ )
Simulated sample size	0.6
Hardware trigger efficiency	0.6
Particle identification efficiencies	0.3
Form-factors	0.2
$\mathcal{B}(\tau^- \rightarrow \mu^-\bar{\nu}_\mu\nu_\tau)$	< 0.1
<b>Total normalization uncertainty</b>	<b>0.9</b>
<b>Total systematic uncertainty</b>	<b>3.0</b>

# $R(D^*)$ hadronic ( $\tau \rightarrow 3\pi\nu_\tau$ )

$$R(D^*) = \mathcal{K}(D^*) \times \frac{\mathcal{B}(B^0 \rightarrow D^{*-} 3\pi)}{\mathcal{B}(B^0 \rightarrow D^{*-} \mu^+ \nu_\mu)}$$
$$\text{with } \mathcal{K}(D^*) = \frac{\mathcal{B}(B^0 \rightarrow D^{*-} \tau^+ \nu_\tau)}{\mathcal{B}(B^0 \rightarrow D^{*-} 3\pi)} = \frac{N_{D^* \tau \nu_\tau}}{N_{D^* 3\pi}} \times \frac{\varepsilon_{D^* 3\pi}}{\varepsilon_{D^* \tau \nu_\tau}} \times \frac{1}{\mathcal{B}(\tau^+ \rightarrow 3\pi(\pi^0) \bar{\nu}_\tau)}$$

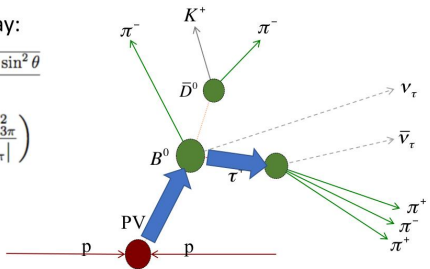
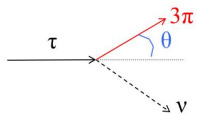
- Signal and normalization modes chosen to have the same final state
- $\mathcal{B}(\tau^+ \rightarrow \pi^+ \pi^- \pi^+ \bar{\nu}_\tau) = (9.31 \pm 0.05)\%$
- $\mathcal{B}(\tau^+ \rightarrow \pi^+ \pi^- \pi^+ \pi^0 \bar{\nu}_\tau) = (4.62 \pm 0.05)\%$
- $N_{D^* 3\pi}$  from unbinned fit to  $D^* 3\pi$  invariant mass
- $N_{D^* \tau \nu_\tau}$  from binned templated fit
- $\mathcal{B}(B^0 \rightarrow D^{*-} 3\pi)$  from [BaBar, PRD94 (2016) 091101] ( $\sim 4\%$  precision)
- $\mathcal{B}(B^0 \rightarrow D^{*-} \mu^+ \nu_\mu)$  from PDG ( $\sim 2\%$  precision)

## Signal reconstruction

- 2-fold ambiguity when reconstructing the  $\tau$  decay:

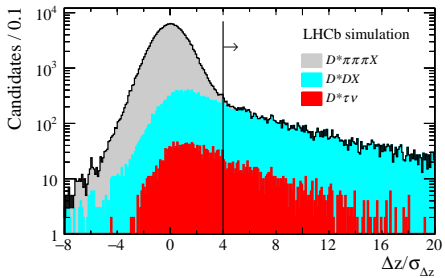
$$|\vec{p}_\tau| = \frac{(m_{3\pi}^2 + m_\tau^2)|\vec{p}_{3\pi}| \cos \theta \pm E_{3\pi} \sqrt{(m_\tau^2 - m_{3\pi}^2)^2 - 4m_\tau^2 |\vec{p}_{3\pi}|^2 \sin^2 \theta}}{2(E_{3\pi}^2 - |\vec{p}_{3\pi}|^2 \cos^2 \theta)}$$

- Can be lifted by choosing  $\theta_{max} = \arcsin \left( \frac{m_\tau^2 - m_{3\pi}^2}{2m_\tau |\vec{p}_{3\pi}|} \right)$



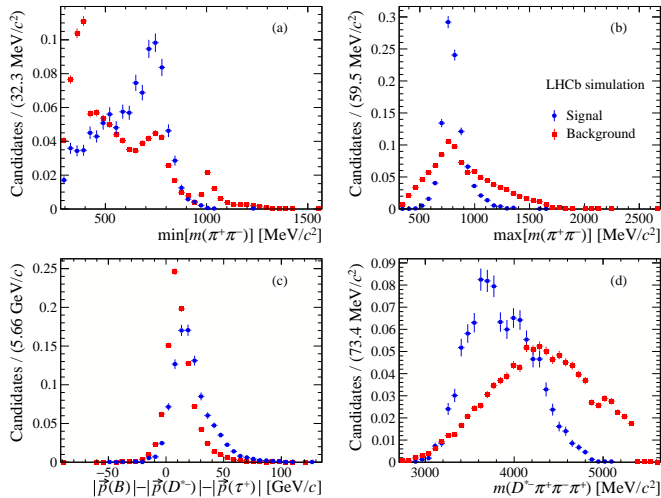
- Same argument for B decay
- Possible to reconstruct rest frame variables such as  $\tau$  decay time and  $q^2$ .
- Negligible biases, and sufficient resolution to preserve good discrimination between signal and background.

# $R(D^*)$ hadronic ( $\tau \rightarrow 3\pi\nu_\tau$ ) [PRD 97,072013 2018]



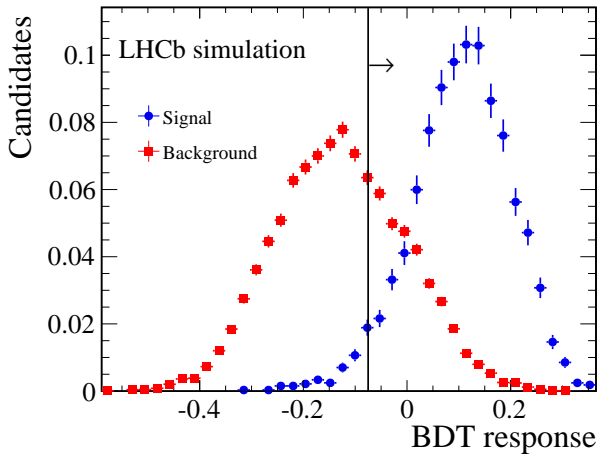
Distribution of the distance between the  $B^0$  vertex and the  $3\pi$  vertex along the beam direction, divided by its uncertainty, obtained using simulation. The grey area corresponds to the prompt background component, the cyan and red areas to double-charm and signal components, respectively. The vertical line shows the  $4\sigma$  requirement used in the analysis to reject the prompt background component

# $R(D^*)$ hadronic ( $\tau \rightarrow 3\pi\nu_\tau$ ). Anti- $D_s^+$ BDT [PRD 97,072013 2018]



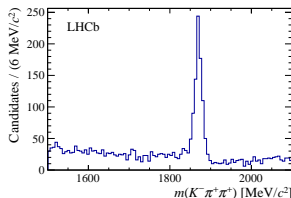
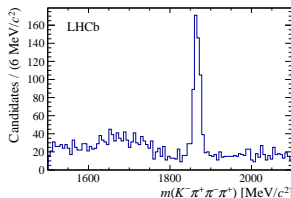
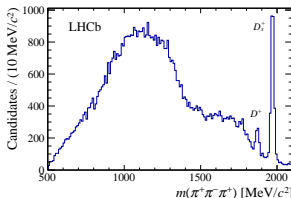
Normalized distributions of (a)  $\min[m(\pi^+\pi^-)]$ , (b)  $\max[m(\pi^+\pi^-)]$ , (c) approximated neutrino momentum reconstructed in the signal hypothesis, and (d) the  $D^* - 3\pi$  mass in simulated samples.

# $R(D^*)$ hadronic ( $\tau \rightarrow 3\pi\nu_\tau$ ) [PRD 97,072013 2018]



Distribution of the BDT response on the signal and background simulated samples.

# $R(D^*)$ hadronic ( $\tau \rightarrow 3\pi\nu_\tau$ ) $D_s^+$ , $D^0$ and $D^+$ control channels [PRD 97,072013 2018]

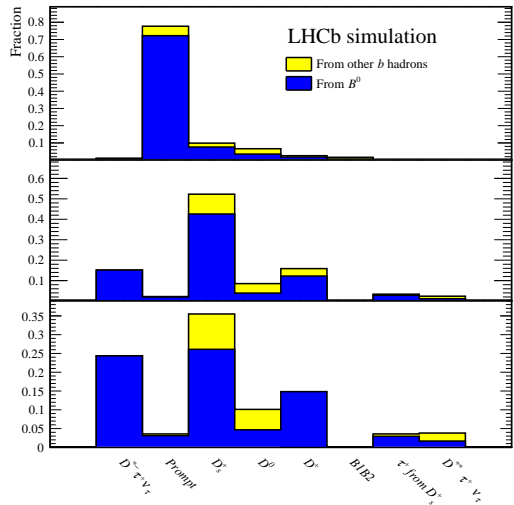


Left: Distribution of the  $3\pi$  mass for candidates after the detached-vertex requirement. The  $D^+$  and  $D_s^+$  mass peaks are indicated.

Center: Distribution of the  $K^-3\pi$  mass for  $D^0$  candidates where a charged kaon has been associated to the  $3\pi$  vertex. (anti-isolation)

Right: Distribution of the  $K^-\pi^+\pi^+$  mass for  $D^+$  candidates passing the signal selection, where the negative pion has been identified as a kaon and assigned the kaon mass. (antiPID)

# $R(D^*)$ hadronic ( $\tau \rightarrow 3\pi\nu_\tau$ ) [PRD 97,072013 2018]



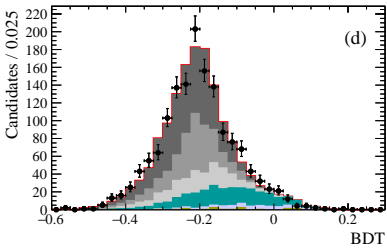
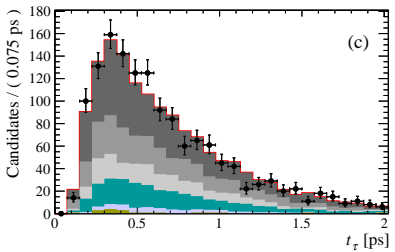
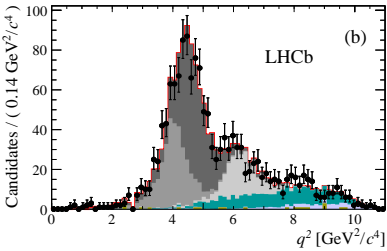
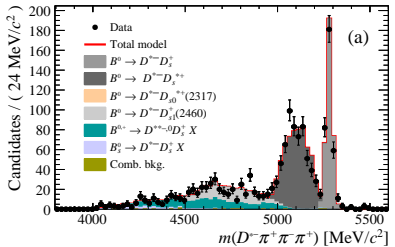
Composition of an inclusive simulated sample where a  $D^*$  — and a  $3\pi$  system have been produced in the decay chain of a  $b\bar{b}$  pair from a  $pp$  collision. Each bin shows the fractional contribution of the different possible parents of the  $3\pi$  system (blue from a  $B^0$ , yellow for other  $b$  hadrons): from signal; directly from the  $b$  hadron (prompt); from a charm parent  $D_s^+, D^0$ , or  $D^+$  meson;  $3\pi$  from a  $B$  and the  $D^0$  from the other  $B$  (B1B2); from  $\tau$  lepton following a  $D_s^+$  decay; from a  $\tau$  lepton following a  $D^{**} \tau^+ \nu_\tau$  decay ( $D^{**}$  denotes here any higher excitation of  $D$  mesons).

(Top) After the initial selection and the removal of spurious  $3\pi$  candidates.

(Middle) For candidates entering the signal fit.

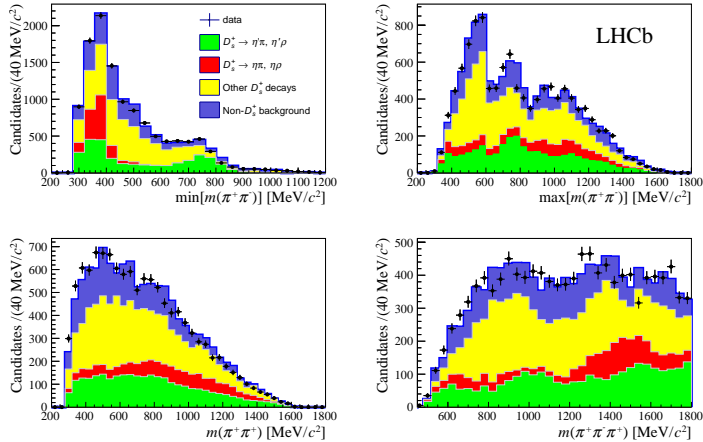
(Bottom) For candidates populating the last 3 bins of the BDT distribution.

# $R(D^*)$ hadronic ( $\tau \rightarrow 3\pi\nu_\tau$ ) Control Sample [PRD 97,072013 2018]



Results from the fit to data for candidates containing a  $D^* \rightarrow D_s^+ \pi^-$  pair, where  $D_s^+ \rightarrow 3\pi$ . The figures correspond to the fit projection on (a)  $m(D^* \rightarrow 3\pi)$ , (b)  $q^2$ , (c)  $3\pi$  decaytime  $t_\tau$  and(d) BDT output distributions.

# $R(D^*)$ hadronic ( $\tau \rightarrow 3\pi\nu_\tau$ ). $D_s^+$ decay model [PRD 97,072013 2018]

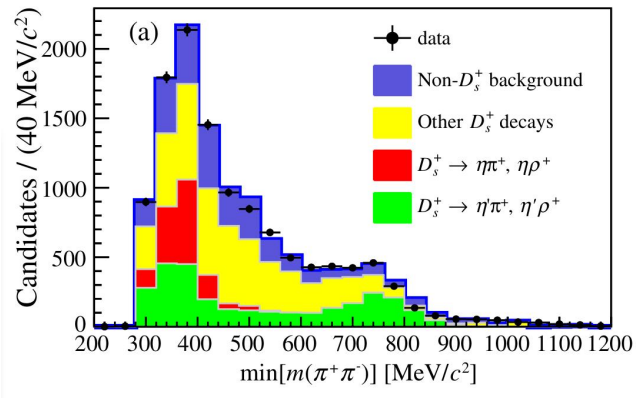


The 4 distributions are fitted simultaneously with a fit model obtained from MC. Sample enriched in  $B \rightarrow D^* \rightarrow D_s^+(X)$  decays, obtained by requiring the BDT output below a certain threshold.

$D_s^+$  decays with at least 1 pion from  $\eta$  (red) or  $\eta'$  (green):  $\eta^{(\prime)}\pi^+, \eta^{(\prime)}\rho^+$

$D_s^+$  decays with at least 1 pion from an intermediate state (IS) other than  $\eta$  or  $\eta'$ :  $\omega$  or  $\phi$  (yellow)

$D_s^+$  decays where none of the 3 pions come from an IS, backgrounds originating from decays not involving the  $D_s^+$  meson:  $K^03\pi, \eta 3\pi, \eta' 3\pi, \omega 3\pi, \phi 3\pi$ , non-resonant (blue).



The  $\tau$  lepton decays through the  $a_1(1260)^+$  resonance, which leads to the  $\rho^0\pi^+$  final. The dominant source of  $\rho^0$  resonances in  $D_s^+$  decays is due to  $\eta' \rightarrow \rho^0\gamma$  decays. It is therefore crucial to control the  $\eta'$  contribution in  $D_s^+$  decays very accurately.

At low  $\min[m(\pi^+\pi^-)]$ , only  $\eta$  and  $\eta'$  (red, green) contributions are peaking:  $\eta \rightarrow \pi^+\pi^-\pi^0$  and  $\eta' \rightarrow \eta\pi^+\pi^-$ . At the  $\rho^0$  mass where the signal lives, only  $\eta'$  contributes:  $\eta' \rightarrow \rho^0\gamma$ . The shape of this  $\eta'$  contribution is precisely known since the  $\eta'$  branching fractions are known to better than 2%. The precise measurement on data of the low-mass excess, which consists only of  $\eta'$  and  $\eta$  candidates, therefore enables the control of the  $\eta'$  contribution in the sensitive  $\rho$  region.

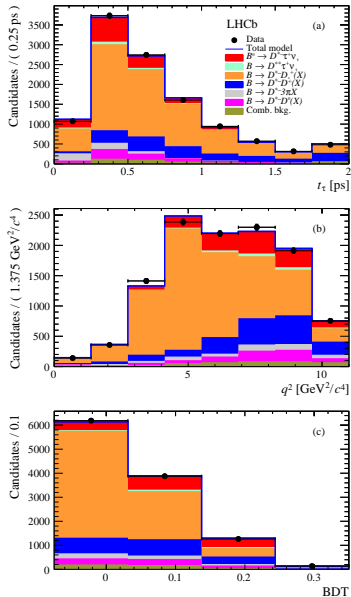
Fits results used to describe the  $D_s^+ \rightarrow 3\pi X$  model in the final fit for  $N_{\text{sig}}$

Results of the fit to the  $D_s^+$  decay model. The relative contribution of each decay and the correction to be applied to the simulation are reported in the second and third columns, respectively.

$D_s^+$ decay	Relative contribution	Correction to simulation
$\eta\pi^+(X)$	$0.156 \pm 0.010$	
	$0.109 \pm 0.016$	$0.88 \pm 0.13$
	$0.047 \pm 0.014$	$0.75 \pm 0.23$
$\eta'\pi^+(X)$	$0.317 \pm 0.015$	
	$0.179 \pm 0.016$	$0.710 \pm 0.063$
	$0.138 \pm 0.015$	$0.808 \pm 0.088$
$\phi\pi^+(X), \omega\pi^+(X)$	$0.206 \pm 0.02$	
	$0.043 \pm 0.022$	$0.28 \pm 0.14$
	$0.163 \pm 0.021$	$1.588 \pm 0.208$
$\eta 3\pi$	$0.104 \pm 0.021$	$1.81 \pm 0.36$
$\eta' 3\pi$	$0.0835 \pm 0.0102$	$5.39 \pm 0.66$
$\omega 3\pi$	$0.0415 \pm 0.0122$	$5.19 \pm 1.53$
$K^0 3\pi$	$0.0204 \pm 0.0139$	$1.0 \pm 0.7$
$\phi 3\pi$	$0.0141$	$0.97$
$\tau^+ (\rightarrow 3\pi(N)\bar{\nu}_\tau) \nu_\tau$	$0.0135$	$0.97$
$X_{\text{nr}} 3\pi$	$0.038 \pm 0.005$	$6.69 \pm 0.94$

# $R(D^*)$ hadronic ( $\tau \rightarrow 3\pi\nu_\tau$ ) [PRD 97,072013 2018]

Projections of the three-dimensional fit on the  
(a)  $3\pi$  decay time  
(b)  $q^2$  and  
(c) BDT output distributions.



Summary of fit components and their corresponding normalization parameters. The first three components correspond to parameters related to the signal.

Fit component	Normalization
$B^0 \rightarrow D^{*-} \tau^+ (\rightarrow 3\pi\bar{\nu}_\tau) \nu_\tau$	$N_{\text{sig}} \times f_{\tau \rightarrow 3\pi\nu}$
$B^0 \rightarrow D^{*-} \tau^+ (\rightarrow 3\pi\pi^0\bar{\nu}_\tau) \nu_\tau$	$N_{\text{sig}} \times (1 - f_{\tau \rightarrow 3\pi\nu})$
$B \rightarrow D^{**-} \tau^+ \nu_\tau$	$N_{\text{sig}} \times f_{D^{**-} \tau \nu}$
$B \rightarrow D^{*-} D^+ X$	$f_{D_s^+} \times N_{D_s}$
$B \rightarrow D^{*-} D^0 X$ different vertices	$f_{D_s^0} \times N_{D^0}^{\text{sv}}$
$B \rightarrow D^{*-} D^0 X$ same vertex	$N_{D^0}^{\text{sv}}$
$B^0 \rightarrow D^{*-} D_s^+$	$N_{D_s} \times f_{D_s^+}/k$
$B^0 \rightarrow D^{*-} D_s^{*+}$	$N_{D_s} \times 1/k$
$B^0 \rightarrow D^{*-} D_{s0}^*(2317)^+$	$N_{D_s} \times f_{D_{s0}^{*+}}/k$
$B^0 \rightarrow D^{*-} D_{s1}(2460)^+$	$N_{D_s} \times f_{D_{s1}^+}/k$
$B^{0,+} \rightarrow D^{**-} D_s^+ X$	$N_{D_s} \times f_{D_s^+ X}/k$
$B_s^0 \rightarrow D^{*-} D_s^+ X$	$N_{D_s} \times f_{(D_s^+ X)_s}/k$
$B \rightarrow D^{*-} 3\pi X$	$N_{B \rightarrow D^* 3\pi X}$
B1B2 combinatorics	$N_{B1B2}$
Combinatoric $D^{*-}$	$N_{\text{not}D^*}$

Fit results for the three-dimensional fit. The constraints on the parameters  $f_{D_s^+}$ ,  $f_{D_{s0}^{*+}}$ ,  $f_{D_{s1}^+}$ ,  $f_{D_s^+ X}$  and  $f_{(D_s^+ X)_s}$  are applied taking into account their correlations.

Parameter	Fit result	Constraint
$N_{\text{sig}}$	$1296 \pm 86$	
$f_{\tau \rightarrow 3\pi\nu}$	0.78	0.78 (fixed)
$f_{D^{**}\tau\nu}$	0.11	0.11 (fixed)
$N_{D_s^0}$	$445 \pm 22$	$445 \pm 22$
$f_{D_s^0}$	$0.41 \pm 0.22$	
$N_{D_s}$	$6835 \pm 166$	
$f_{D_s^+}$	$0.245 \pm 0.020$	
$N_{B \rightarrow D^* 3\pi X}$	$424 \pm 21$	$443 \pm 22$
$f_{D_s^+}$	$0.494 \pm 0.028$	$0.467 \pm 0.032$
$f_{D_{s0}^{*+}}$	$0_{-0.000}^{+0.010}$	$0_{-0.000}^{+0.042}$
$f_{D_{s1}^+}$	$0.384 \pm 0.044$	$0.444 \pm 0.064$
$f_{D_s^+ X}$	$0.836 \pm 0.077$	$0.647 \pm 0.107$
$f_{(D_s^+ X)_s}$	$0.159 \pm 0.034$	$0.138 \pm 0.040$
$N_{B1B2}$	197	197 (fixed)
$N_{\text{not}D^*}$	243	243 (fixed)

$$R(D^*) = 0.291 \pm 0.019(\text{stat}) \pm 0.026(\text{syst}) \pm 0.013(\text{ext})$$

Relative systematics uncertainties:

Source	$\delta R(D^{*-})/R(D^{*-})[\%]$
Simulated sample size	4.7
Empty bins in templates	1.3
Signal decay model	1.8
$D^{**} \tau \nu$ and $D_s^{**} \tau \nu$ feeddowns	2.7
$D_s^+ \rightarrow 3\pi X$ decay model	2.7
$B \rightarrow D^{*-} D_s^+ X$ , $B \rightarrow D^{*-} D^+ X$ , $B \rightarrow D^{*-} D^0 X$ backgrounds	3.9
Combinatorial background	0.7
$B \rightarrow D^{*-} 3\pi X$ background	2.8
Efficiency ratio	3.9
Normalization channel efficiency (modeling of $B^0 \rightarrow D^{*-} 3\pi$ )	2.0
Total systematic uncertainty	9.1

$$R(D^*) = 0.291 \pm 0.019(\text{stat}) \pm 0.026(\text{syst}) \pm 0.013(\text{ext})$$

List of the individual systematic uncertainties for  $R(D^*)$ :

Contribution	Value in %
$\mathcal{B}(\tau^+ \rightarrow 3\pi\nu_\tau) / \mathcal{B}(\tau^+ \rightarrow 3\pi(\pi^0)\nu_\tau)$	0.7
Form factors (template shapes)	0.7
Form factors (efficiency)	1.0
$\tau$ polarization effects	0.4
Other $\tau$ decays	1.0
$B \rightarrow D^{**} \tau^+ \nu_\tau$	2.3
$B_s^0 \rightarrow D_s^{**} \tau^+ \nu_\tau$ feed-down	1.5
$D_s^+ \rightarrow 3\pi X$ decay model	2.5
$D_s^+, D^0$ and $D^+$ template shape	2.9
$B \rightarrow D^* - D_s^+(X)$ and $B \rightarrow D^* - D^0(X)$ decay model	2.6
$D^* - 3\pi X$ from $B$ decays	2.8
Combinatorial background (shape + normalization)	0.7
Bias due to empty bins in templates	1.3
Size of simulation samples	4.1
Trigger acceptance	1.2
Trigger efficiency	1.0
Online selection	2.0
Offline selection	2.0
Charged-isolation algorithm	1.0
Particle identification	1.3
Normalization channel	1.0
Signal efficiencies (size of simulation samples)	1.7
Normalization channel efficiency (size of simulation samples)	1.6
Normalization channel efficiency (modeling of $B^0 \rightarrow D^* - 3\pi$ )	2.0
Total uncertainty	9.1

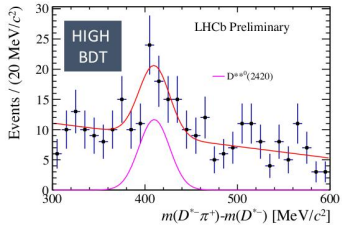
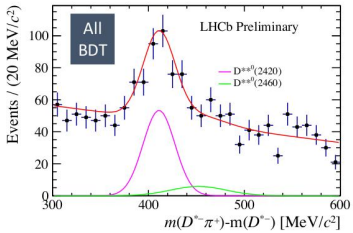
## Additional cross-checks: $X_b \rightarrow D^{**}\tau\nu$

- $B^0 \rightarrow D^{**}\tau\nu$  and  $B^+ \rightarrow D^{**0}\tau\nu$  constitute potential feed-down to the signal.
- $D^{**}(2420)^0$  is reconstructed using its decay to  $D^{*+}\pi^-$  as a cross-check.
- The observation of the  $D^{**}(2420)^0$  peak allows to compute the  $D^{**}3\pi$  BDT distribution and to deduce a  $D^{**}\tau\nu$  upper limit. This upper limit is consistent with the theoretical prediction.
- Subtract contribution of  $(11 \pm 0.04)\%$  due to  $D^{**}\tau\nu$  feed-down; resulting systematic uncertainty of 2.3%.

06/07/17

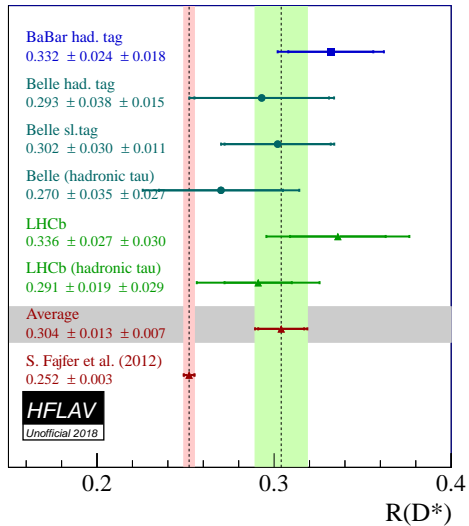
Concezio Bozzi -- Recent LHCb results on SL decays

LHCb-PAPER-2017-017



# $R(D^*)$ HFLAV

Unofficial! Average not updated with latest LHCb Hadronic result!



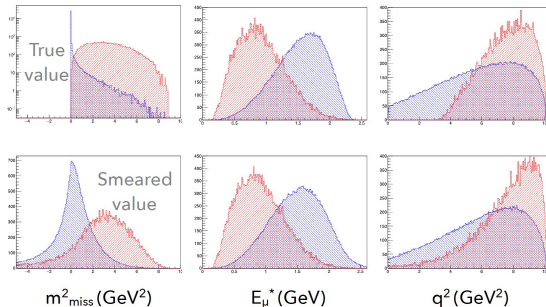
[HFLAV]

$B_c \rightarrow J/\psi \tau \nu : R_{J/\psi}$

- Generalization of  $R(D^*)$  to  $B_c^+$

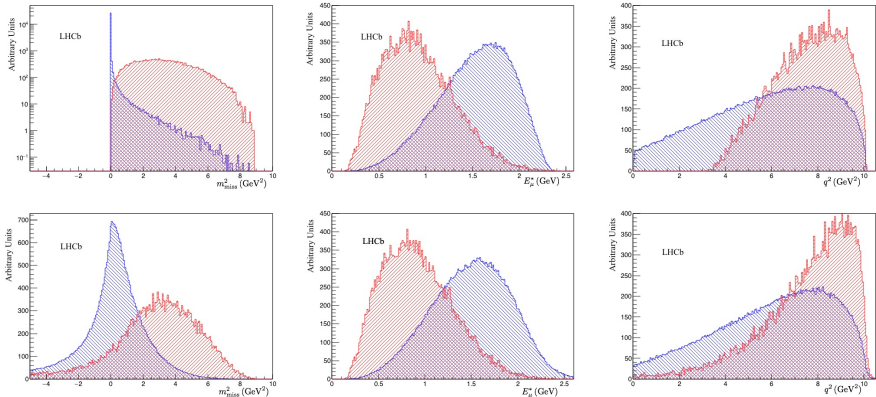
$$R(J/\psi) = \frac{\mathcal{B}(B_c^+ \rightarrow J/\psi \tau^+ \nu_\tau)}{\mathcal{B}(B_c^+ \rightarrow J/\psi \mu^+ \nu_\mu)}$$

- $B_c^+$  decay form factors unconstrained experimentally: theoretical prediction not yet precise 0.25-0.28
- Reconstruct signal with  $\tau \rightarrow \mu \nu_\mu \nu_\tau$  (17%)
- Like in  $R(D^*)$ , use  $m_{\text{miss}}^2$ ,  $E_\mu^*$  and  $q^2$ . Add information from  $B_c^+$  decay time
- Imperfect reconstruction due to missing neutrinos. The broad shapes of the distributions are smeared but their discriminating power is preserved



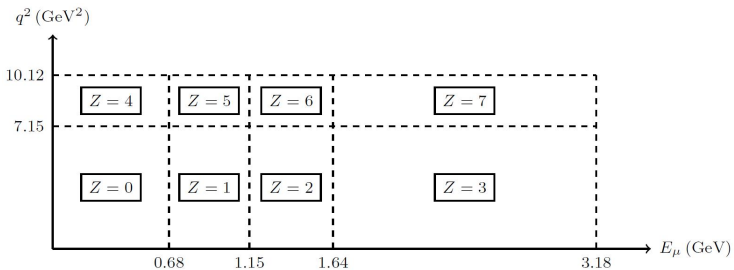
## Systematic uncertainties

Model uncertainties	Size (eff. corrected) ( $\times 10^{-2}$ )
Uncertainty due to finite size of simulation data	8.0
$B_c^+ \rightarrow J/\psi$ form factors	12.1
$B_c^+ \rightarrow \psi(2S)$ form factors	3.2
Bias correction	5.4
$B_c^+ \rightarrow J/\psi H_c X$ cocktail composition	3.6
$Z$ binning strategy	5.6
Misidentification background strategy	5.4
Combinatorial background cocktail	4.5
Combinatorial $J/\psi$ sideband scaling	0.9
Empirical reweighting	1.6
Semitauonic $\psi(2S)$ and $\chi_c$ feed-down	0.9
Fixing $A_2(q^2)$ slope to zero	0.3
Efficiency ratio	0.6
$\mathcal{B}(\tau \rightarrow \mu \nu \nu)$	0.2
$B_c^+$ lifetime	included in stat.
<b>Total systematic uncertainty</b>	<b>17.7</b>
<b>Statistical uncertainty</b>	<b>17.3</b>

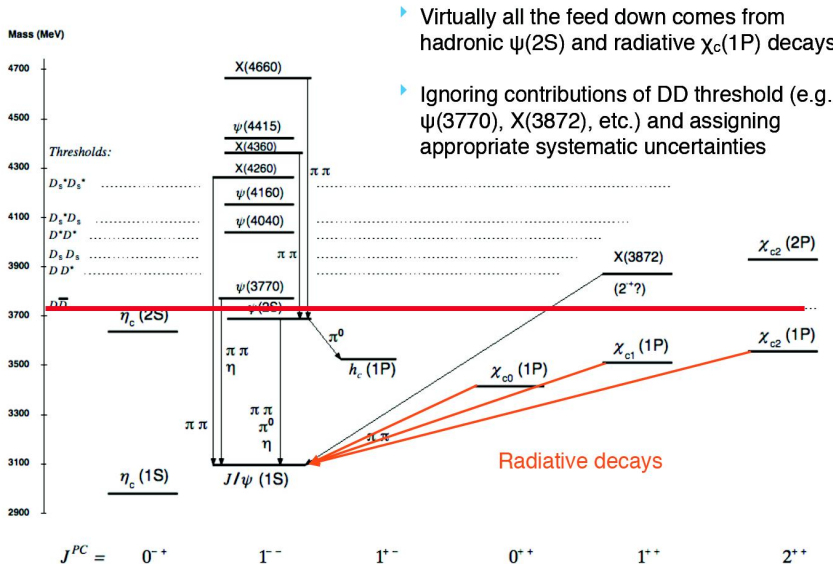


For each fit variable (save the mostly unaltered decay time), the distributions of the quantity calculated using the simulated true  $B_c^+$  momentum and the approximated momentum are shown. In each plot, the normalization  $B_c^+ \rightarrow J/\psi \mu^+ \nu_\mu$  decay is shown in blue, while the signal  $B_c^+ \rightarrow J/\psi \tau^+ \nu_\tau$  is shown in red. The smearing induced by the rest frame approximation does not wash out the discriminating power of these variables.

Trick to make a 3D fit with 4 variables: the  $Z$  variable merge information from  $q^2$  and  $E_\mu^*$



## Charmonium feed-down background



## About the Form Factors (largest systematic uncertainty)

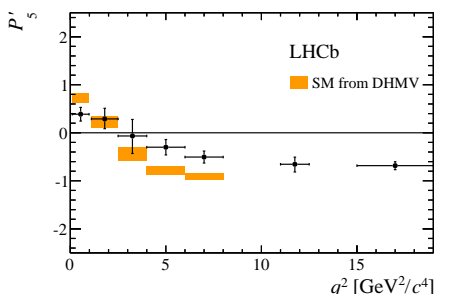
The templates are derived from simulation for the signal and the normalization modes, which requires knowledge of the  $B_c \rightarrow J/\psi$  form factors. These have not yet been precisely determined and the theoretical predictions, e.g. those from Kiselev, Ebert, Faustov, and Galkin have been tested against data. Thus, for this measurement, the shared form factors for the signal and normalization channels are determined directly from the data by employing a z-expansion parametrization inspired by [BCL] to fit a sub-sample of the data.

# Other analyzes

# The Decay $B^0 \rightarrow K^{*0} \mu^+ \mu^-$

- Measured by 4 different experiments: Belle, LHCb, ATLAS, CMS
- Most precise measurement from LHCb

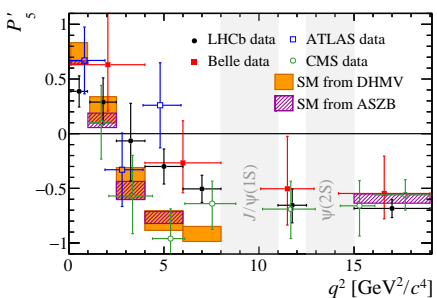
## LHCb Only



LHCb, JHEP02 (2016) 104,

arxiv:1512.04442

## All Together

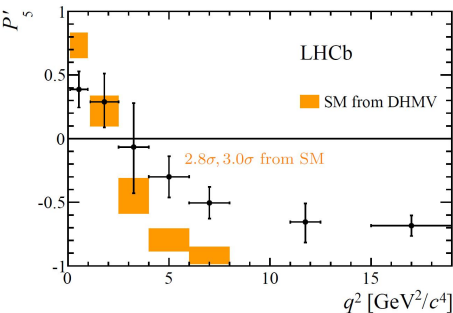
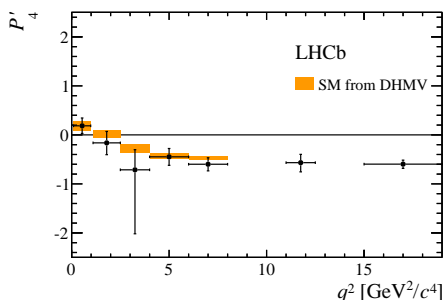


Belle, arxiv:1604.04042

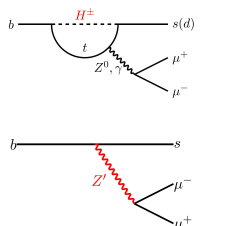
ATLAS, ATLAS-CONF-2017-023

CMS, CMS-PAS-BPH-15-008

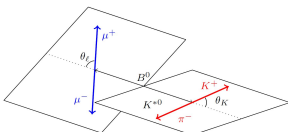
- Significance:  $3.4\sigma$
- Ongoing discussion about the interpretation and theory predictions
- Situation is not as clear cut as for the  $R$ -measurements



- Mainly compatible with the SM except one angular variable
- Local  $2.8\text{--}3.0\sigma$  discrepancy with SM prediction in bins  $q^2 \equiv m_{\mu\mu}^2 \in [4, 8] \text{ GeV}^2/c^4$  of  $P'_5$
- LHCb fit of the EW penguin Wilson coeff  $C_9$ , including  $S_3 - S_9, F_L, A_{FB}$ :  $3.4\sigma$  from SM
- Theoretical work ongoing to better understand this effect: NP or unexpectedly large hadronic effect?  
see e.g. [Descotes-Genon et al., arXiv:1510.04239]
- Channel also studied by BaBar [arXiv:1508.07960], Belle [PRL 103, 171801], CMS [PLB 753(2016)424], ATLAS [ATLAS-CONF-2013-038] and CDF [PRL 108, 081807]



- Same motivations as  $B^- \rightarrow K^- \ell^+ \ell^-$ .  
Same SM loops, but with a **vector** in the final state, sensitive to  $C_7^{(\prime)}$ ,  $C_9^{(\prime)}$  and  $C_{10}^{(\prime)}$
- Complicated angular analysis with many observables:



$$\frac{1}{d\Gamma/dq^2} \frac{d^4\Gamma}{d\cos\theta_\ell d\cos\theta_K d\phi dq^2} = \frac{9}{32\pi} \left[ \frac{3}{4}(1-F_L) \sin^2\theta_K + F_L \cos^2\theta_K + \frac{1}{4}(1-F_L) \sin^2\theta_K \cos 2\theta_\ell - F_L \cos^2\theta_K \cos 2\theta_\ell + S_3 \sin^2\theta_K \sin^2\theta_\ell \cos 2\phi + S_4 \sin 2\theta_K \sin 2\theta_\ell \cos\phi + S_5 \sin 2\theta_K \sin\theta_\ell \cos\phi + S_6 \sin^2\theta_K \cos\theta_\ell + S_7 \sin 2\theta_K \sin\theta_\ell \sin\phi + S_8 \sin 2\theta_K \sin 2\theta_\ell \sin\phi + S_9 \sin^2\theta_K \sin^2\theta_\ell \sin 2\phi \right]$$

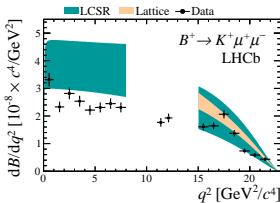
- Can parameterize the angular coeff to be largely free of form factor uncertainties

[Descotes-Genon et al, JHEP, 1305:137, (2013)]

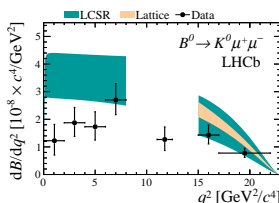
e.g.  $P'_5 = \frac{S_5}{\sqrt{F_L(1-F_L)}}$  where  $F_L$  is the fraction of longitudinal polarization

# Other $b \rightarrow s\mu^+\mu^-$ Branching Fractions

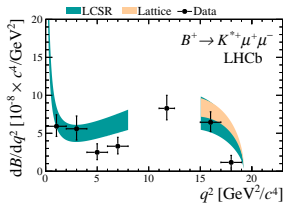
$B^+ \rightarrow K^+\mu^+\mu^-$



$B_d^0 \rightarrow K^{*0}\mu^+\mu^-$



$B^+ \rightarrow K^{*+}\mu^+\mu^-$



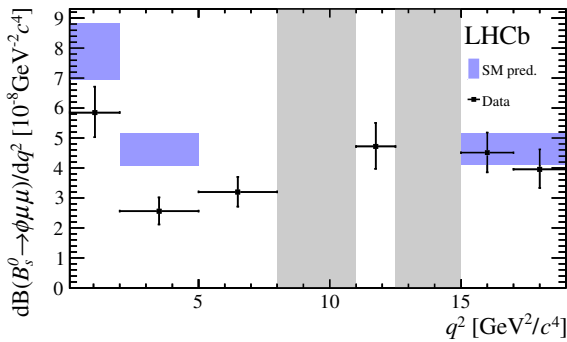
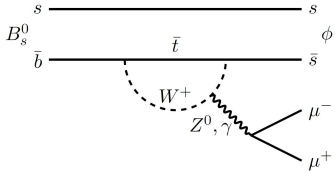
- Also used for  $R_K$

- Also used for  $R_{K^*}$

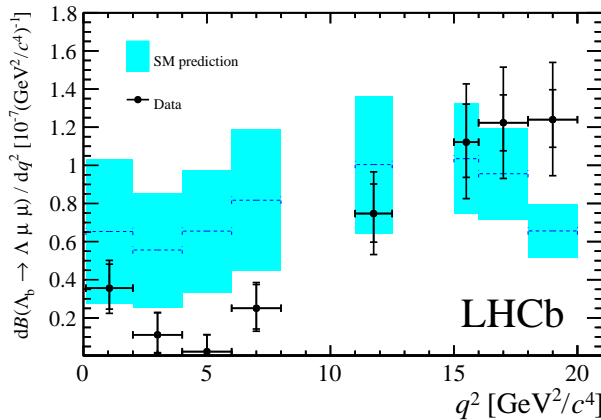
LHCb, JHEP06(2014)133, arxiv:1403.8044

- Measure branching fractions as a function of  $q^2$
  - All are below the theory predictions
- ⇒ Same trend as for  $R_K$  and  $R_{K^*}$

- Similar to  $B^0 \rightarrow K^* \mu^+ \mu^-$ , but not self-tagged (no CP observable accessible)
- Narrow  $\phi$  resonance gives clean signal peak
- Full angular analysis
- At low  $q^2$ , BR also below SM [Altmannshofer, Straub, EPJ C75 (2015) 382], [Bharucha et al, arXiv:1503.05534]

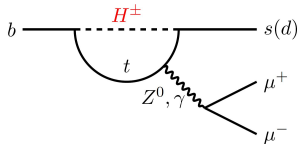


- Similar to  $B^0 \rightarrow K^* \mu^+ \mu^-$
- Baryonic system provides sensitivity to additional observables
- Rate still too low to perform a full angular analysis.
- Again, BR lower than SM at low  $q^2$ : deficit of muons?

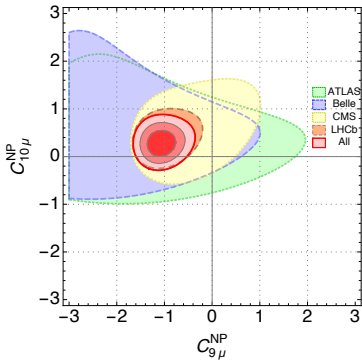


SM from [Detmold et al., PRD 87, (2013) 074502]

# Neutral current anomalies $b \rightarrow s\ell\ell$

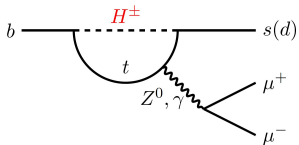


- Several measurements involving  $b \rightarrow s\ell\ell$ , ( $\ell = \mu, e$ ) deviate from their SM expectation ( $2 - 3\sigma$ )
- $R_K = \mathcal{B}(B^+ \rightarrow K^+ \mu^+ \mu^-)/\mathcal{B}(B^+ \rightarrow K^+ e^+ e^-)$ ,  $R_{K^*}$ , BR of  $B^0 \rightarrow K^* \mu^+ \mu^-$ ,  $B_s^0 \rightarrow \phi \mu^+ \mu^-$ ,  $\Lambda_b \rightarrow \Lambda^0 \mu^+ \mu^-$ ,  $P'_5$
- The combined effect of these “small” deviations point towards the same direction:  $C_{9\mu}^{\text{NP}} = -1$ , implying **violation of the leptonic universality  $\mu \neq e$** . Significance of global fits  $\sim 5\sigma$  [Capdevila et al., JHEP 1801 (2018) 093]
- Deficit of muons? Theoretical uncertainties or experimental?

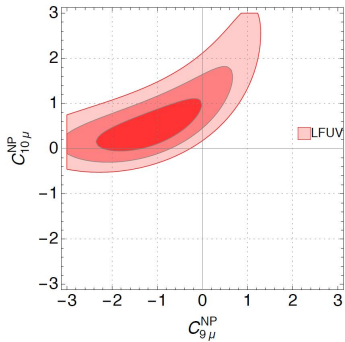


[Capdevila et al., JHEP 1801 (2018) 093]

# Neutral current anomalies $b \rightarrow s\ell\ell$



- Several measurements involving  $b \rightarrow s\ell\ell$ , ( $\ell = \mu, e$ ) deviate from their SM expectation ( $2 - 3\sigma$ )
- $R_K = \mathcal{B}(B^+ \rightarrow K^+ \mu^+ \mu^-)/\mathcal{B}(B^+ \rightarrow K^+ e^+ e^-)$ ,  $R_{K^*}$
- The combined effect of these “small” deviations point towards the same direction:  $C_{9\mu}^{\text{NP}} = -1$ , implying **violation of the leptonic universality**  $\mu \neq e$ . Significance of global fits, if using only “LFU” observables: between 3 and  $4\sigma$  [Capdevila et al., JHEP 1801 (2018) 093]
- Deficit of muons? Theoretical uncertainties or experimental?



[Capdevila et al., JHEP 1801 (2018) 093]

# Few searches for Lepton Flavor Violating decays

- $B_{(s)}^0 \rightarrow e^\pm \mu^\mp$   
[LHCb, PRL 108, 231801 (2012)]:  
 $\mathcal{B}(B^0 \rightarrow e^\pm \mu^\mp) < 2.8 \times 10^{-9}$  at 90% CL  
 $\mathcal{B}(B_s^0 \rightarrow e^\pm \mu^\mp) < 1.1 \times 10^{-9}$  at 90% CL  
20 times better than previous limits. Constraints on leptoquarks
- $D^0 \rightarrow e^\pm \mu^\mp$   
[LHCb, PLB 745 (2016) 167] Set a limit 20 times better than Belle's one:  
 $\mathcal{B}(D^0 \rightarrow e^\pm \mu^\mp) < 1.3 \times 10^{-8}$  at 90% CL
- $\tau^- \rightarrow \mu^- \mu^+ \mu^-$   
Best limits by Belle and BaBar. Also [LHCb, JHEP 1502 (2015) 121]

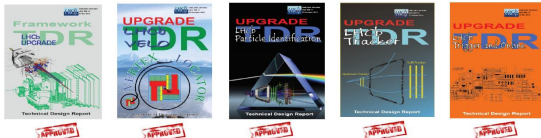
# LHCb and future plans

# LHCb plans

- Run 2 (2016-2018):  $5 \text{ fb}^{-1}$  at  $\sqrt{s} = 13 \text{ TeV}$ , improved trigger
- Some major experimental measurements (e.g.  $\gamma$ ,  $B_s^0 \rightarrow \phi\phi$ ) are not yet at the level of theoretical prediction
- Above a luminosity of  $\sim 4 \times 10^{32} \text{ cm}^{-2} \text{ s}^{-1}$ , LHCb efficiency to trigger hadronic modes saturates, because of the L0-trigger bottleneck which can not cope with more than 1 MHz output rate.

⇒ upgrade 1 of the LHCb experiment in 2019:

- Full software trigger: read all detector at 40 MHz →  $\times 2$  efficiency for hadronic final state.
- Luminosity up to  $2 \times 10^{33} \text{ cm}^{-2} \text{ s}^{-1}$ , new challenges: high pile-up, large occupancies, radiation damages
- Detector upgrades: VELO (pixels), tracker (Silicon strips and scintillating fibers), RICH (multi-anode PMTs), CALO & MUON (new electronics), ...
- Aim to collect  $\sim 50 \text{ fb}^{-1}$ . Annual yields wrt published analyses:  
 $\times 10$  for muonic final states and  $\times 20$  for hadronic modes.



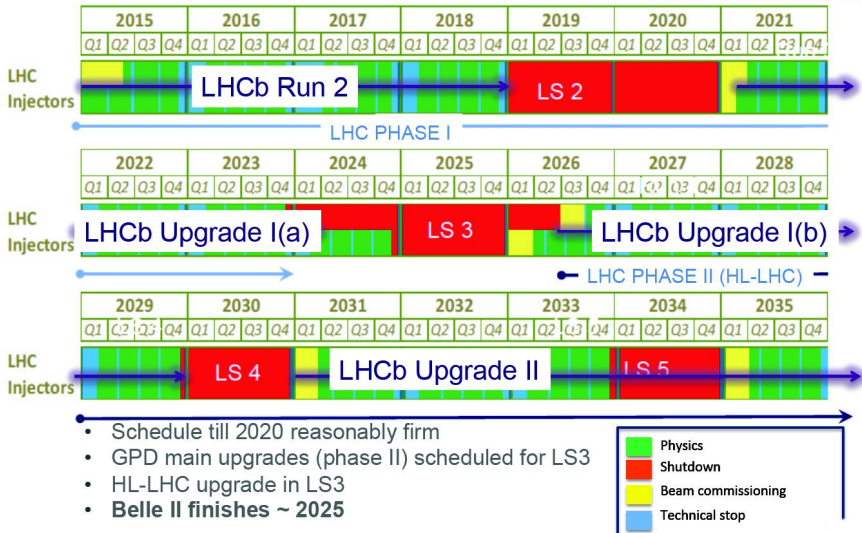
# Expected performances of LHCb upgrade 1

[LHCb-PUB-2014-040]

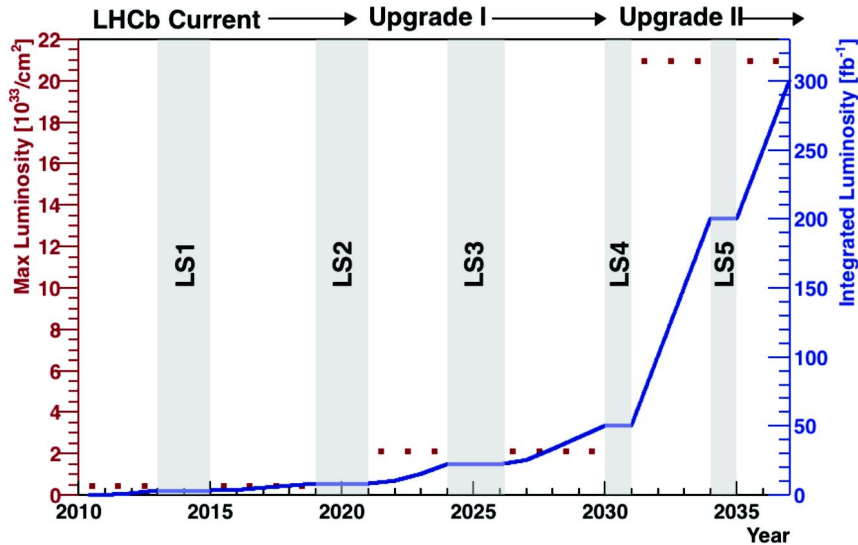
Type	Observable	LHC Run 1	LHCb 2018	LHCb upgrade	Theory
$B_s^0$ mixing	$\phi_s(B_s^0 \rightarrow J/\psi \phi)$ (rad)	0.049	0.025	<b>0.009</b>	$\sim 0.003$
	$\phi_s(B_s^0 \rightarrow J/\psi f_0(980))$ (rad)	0.068	0.035	<b>0.012</b>	$\sim 0.01$
	$A_{sl}(B_s^0) (10^{-3})$	2.8	1.4	<b>0.5</b>	0.03
Gluonic penguin	$\phi_s^{\text{eff}}(B_s^0 \rightarrow \phi\phi)$ (rad)	0.15	0.10	<b>0.018</b>	0.02
	$\phi_s^{\text{eff}}(B_s^0 \rightarrow K^{*0}\bar{K}^{*0})$ (rad)	0.19	0.13	<b>0.023</b>	$< 0.02$
	$2\beta^{\text{eff}}(B_s^0 \rightarrow \phi K_s^0)$ (rad)	0.30	0.20	<b>0.036</b>	0.02
Right-handed currents	$\phi_s^{\text{eff}}(B_s^0 \rightarrow \phi\gamma)$ (rad)	0.20	0.13	<b>0.025</b>	$< 0.01$
	$\tau^{\text{eff}}(B_s^0 \rightarrow \phi\gamma)/\tau_{B_s^0}$	5%	3.2%	<b>0.6%</b>	0.2 %
Electroweak penguin	$S_3(B^0 \rightarrow K^{*0}\mu^+\mu^- ; 1 < q^2 < 6 \text{ GeV}^2/c^4)$	0.04	0.020	<b>0.007</b>	0.02
	$q_0^2 A_{FB}(B^0 \rightarrow K^{*0}\mu^+\mu^-)$	10%	5%	<b>1.9%</b>	$\sim 7\%$
	$A_I(K\mu^+\mu^- ; 1 < q^2 < 6 \text{ GeV}^2/c^4)$	0.09	0.05	<b>0.017</b>	$\sim 0.02$
	$\mathcal{B}(B^+ \rightarrow \pi^+\mu^+\mu^-)/\mathcal{B}(B^+ \rightarrow K^+\mu^+\mu^-)$	14%	7%	<b>2.4%</b>	$\sim 10\%$
Higgs penguin	$\mathcal{B}(B_s^0 \rightarrow \mu^+\mu^-)(10^{-9})$	1.0	0.5	<b>0.19</b>	0.3
	$\mathcal{B}(B^0 \rightarrow \mu^+\mu^-)/\mathcal{B}(B_s^0 \rightarrow \mu^+\mu^-)$	220%	110%	<b>40%</b>	$\sim 5\%$
Unitarity triangle angles	$\gamma(B \rightarrow D^{(*)}K^{(*)})$	7°	4°	<b>0.9°</b>	negligible
	$\gamma(B_s^0 \rightarrow D_s^{\mp}K^{\pm})$	17°	11°	<b>2.0°</b>	negligible
	$\beta(B^0 \rightarrow J/\psi K_s^0)$	1.7°	0.8°	<b>0.31°</b>	negligible
Charm $\mathcal{CP}$ violation	$A_{\Gamma}(D^0 \rightarrow K^+K^-)(10^{-4})$	3.4	2.2	<b>0.4</b>	–
	$\Delta A_{\mathcal{CP}}(10^{-3})$	0.8	0.5	<b>0.1</b>	–

- $\phi_s^{\text{eff}}(B_s^0 \rightarrow \phi\phi)$  with a precision of 0.018
- $\gamma$  with a precision below 1°

# Planning LHC 2035



# Planning LHC 2035



# The LHCb detector

[JINST 3 (2008 S08005)]

- Single-arm forward spectrometer:

- **Tracking system**

IP resolution  $\sim 15\mu\text{m}$  (at high  $p_{\text{T}}$ )

$\delta p/p \sim 0.45\%$

- **RICH system**

Very good  $K - \pi$  identification for  
 $p \sim 2 - 100 \text{ GeV}/c$

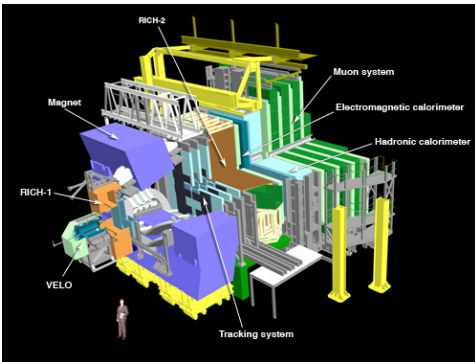
- **Calorimeters**

Energy measurement, identify  $\pi^0, \gamma, e$   
+ trigger

- **Muon detector**

muon identification + trigger

- Integrated lumi  $1 \text{ fb}^{-1}$  (2011),  $2 \text{ fb}^{-1}$  (2012)  
Instantaneous lumi  $\sim 1 - 4 \times 10^{32} \text{ cm}^{-2} \text{s}^{-1}$



# LHCb: general-purpose detector at the LHC

LHCb is a forward spectrometer installed on the LHC, with a broad physics program, continually expanding:

- CKM and CP violation
- Rare decays
- Charm physics
- Kaon physics
- Spectroscopy in  $pp$  interactions
- Heavy quark production
- Exotica searches (tetraquarks, pentaquarks, dark sector, ...)
- Electroweak and QCD measurements in the forward region
- Higgs and top
- Heavy ion physics ( $p$ -Pb, Pb-Pb), fixed-target collisions (He, Ne, Ar).

Examples of publications, well beyond  $b$ -physics:

[Search for Majorana neutrinos in  $B^- \rightarrow \pi \mu^+ \mu^+$  decays, PRL 2014],

[Search for dark photons produced in 13 TeV  $pp$  collision, PRL 2018],

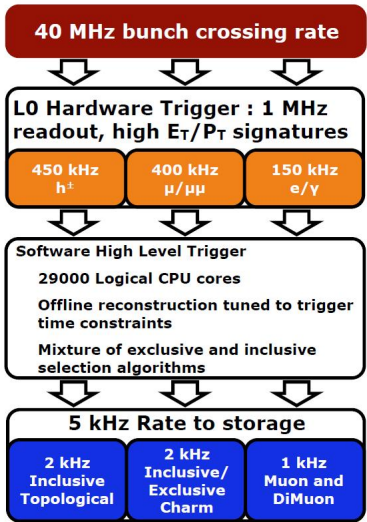
[Measurement of forward top pair production in the dilepton channel in  $pp$  collisions at  $\sqrt{s} = 13$  TeV, 1803.05188],

[Measurements of long-range near-side angular correlations in  $\sqrt{s_{NN}} = 5$  TeV proton-lead collisions in the forward region, PLB 2016],

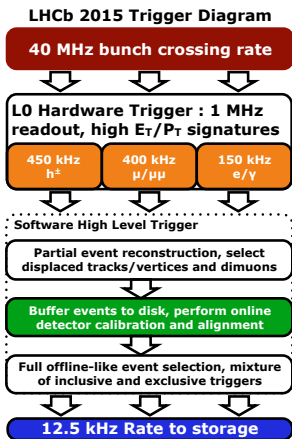
[Limits on neutral Higgs boson production in the forward region in  $pp$  collisions at  $\sqrt{s} = 7$  TeV, JHEP 2013]

# The LHCb Trigger in 2011–2012

- L0 hardware trigger:
  - Find lepton, hadron with high  $p_T$
  - Reduce the rate from 40 MHz to 1 MHz
- HLT1 software trigger:
  - Finds vertices in VELO
  - Tracks with high IP &  $p_T$
- HLT2 software trigger:
  - Reconstruct all tracks in event
  - Select inclusive/exclusive b-hadrons
  - Output rate = 5 kHz



# Trigger in 2015



# LHCb upgrade trigger (2020)

## LHCb Upgrade Trigger Diagram

**30 MHz inelastic event rate,  
event building at full rate**



**LLT: 15-30 MHz output rate,  
select high  $E_T/p_T$  ( $h^\pm/\mu/\gamma$ )**

### Software High Level Trigger

Full event reconstruction, inclusive and exclusive kinematic/geometric selections

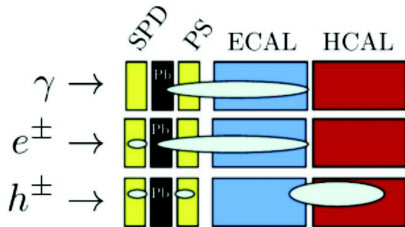
### Run-by-run detector calibration

Add offline precision particle identification and track quality information to selections



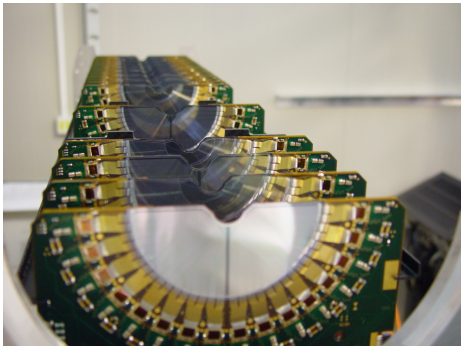
**2-10 GB/s rate to storage**

# LHCb Calorimeters



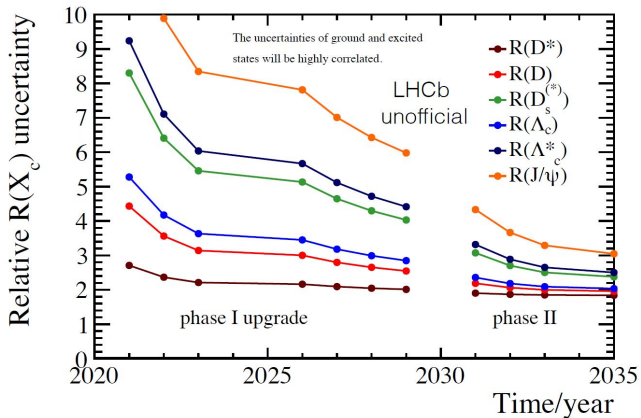
- Composed of a Scintillating Pad Detector (SPD), a Preshower (PS), an electromagnetic calorimeter (ECAL) and a hadronic calorimeter (HCAL)
- The SPD and the PS consist of a plane of scintillator tiles (2.5 radiation lengths, but to only  $\sim 6\%$  hadronic interaction lengths)
- The ECAL has shashlik-type construction, i.e. a stack of alternating slices of lead absorber and scintillator (25 radiation lengths)
- The HCAL is a sampling device made from iron and scintillator tiles being orientated parallel to the beam axis (5.6 interaction lengths)

# LHCb Vertex detector



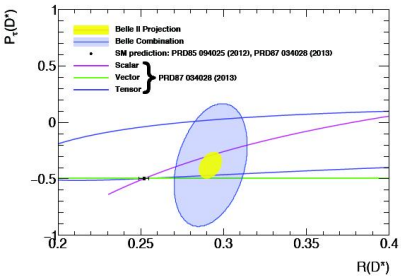
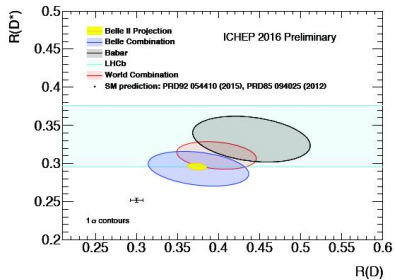
21 (+2) Silicon disks (42 +4 modules).  
8.2 mm from the beam axis. 300  $\mu\text{m}$  thick. Strip pitches 37–97  $\mu\text{m}$

# Some LHCb expectations on $R(X_c)$



- Above are only crude estimates, to be refined soon.
- Other observables than  $R(X_c)$  available to study NP: angles,  $BR(q^2)$ , polarization, ...
- Samples with high signal purity can be obtained, in particular using hadronic  $\tau$  decays

## Belle II Projections



	$\Delta R(D) [\%]$			$\Delta R(D^*) [\%]$		
	Stat	Sys	Total	Stat	Sys	Total
Belle 0.7 ab <sup>-1</sup>	14	6	16	6	3	7
Belle II 5 ab <sup>-1</sup>	5	3	6	2	2	3
Belle II 50 ab <sup>-1</sup>	2	3	3	1	2	2

- SL- & Had- tag full sim sensitivity studies in progress.
- Projections based on Belle + assumed  $R(D)_{SL}$  precision
- SL background modelling will dominate error @ 50 ab<sup>-1</sup>.

